eLife

Reviewed Preprint
v1 • November 13, 2025
Not revised

Reviewed Preprint
v2 • May 18, 2026
Revised by authors

For correspondence:
labwilliams@gmail.com
hchen@uthsc.edu

Competing interests: No competing interests declared

Funding: See page 34

Reviewing editor: Jonathan Flint, University of California, Los Angeles, United States

Acute opioid responses are modulated by dynamic interactions of *Oprm1* and *Fgf12*

Paige M Lemen[1], Yanning Zuo[2], Alexander S Hatoum[3], Price E Dickson[4], Guy Mittleman[5], Arpana Agrawal[3], Benjamin C Reiner[6], Wade Berrettini[6], David G Ashbrook[1], Mustafa Hakan Gunturkun[1], Xusheng Wang[1], Megan K Mulligan[1], Caleb J Browne[7], Eric J Nestler[7], Francesca Telese[2], Robert W Williams[1] ✉, Hao Chen[1] ✉

[1]University of Tennessee Health Science Center, Memphis, United States • [2]University of California San Diego, San Diego, United States • [3]Washington University, St Louis, United States • [4]Marshall University, Huntington, United States • [5]Ball State University, Muncie, United States • [6]University of Pennsylvania, Philadelphia, United States • [7]Nash Family Department of Neuroscience and Friedman Brain Institute, Icahn School of Medicine at Mount Sinai, New York, United States

eLife Assessment

This study integrates large-scale behavioral, genetic, and molecular analyses in animal models to investigate morphine response. Utilizing high-quality, time-series Quantitative Trait Loci (QTL) mapping, the work provides **compelling** evidential support for novel, time-dependent genetic interactions (epistasis). A **fundamental** result of this rigorous analysis is the discovery of a novel Oprm1-Fgf12-MAPK signaling pathway, which offers new insights into the mechanisms of opioid sensitivity.

https://doi.org/10.7554/eLife.108845.2.sa4

Abstract

Exploring the molecular genetic cascades responsible for behavioral responses to opioids can improve our understanding of drug use initiation. We generated high-precision time-series data for 105 morphine-and naloxone-related traits across ~700 young adult BXD mice (64 diverse strains and both sexes) for 3 hours after a single morphine injection. Variations in responses were mapped using high-precision genome sequencing-based genotypes. The initial locomotor responses to morphine mapped precisely to the μ opioid receptor gene (*Oprm1*) on chromosome (Chr) 10 with a peak linkage of 12.4 (-logP, genome-wide significance level is approximately 3.8). The *B* allele inherited from C57BL/6J was associated with up to 60% higher activity. This effect climaxed at 75 min but was exhausted by 160 min. A second major modulator of opioid-induced locomotion emerged after approximately 100 min. This locus, also associated with a high *B* allele, was located on Chr 16 with peak linkage of 10.6 (-logP) in females. This locus included only one compelling candidate, fibroblast growth factor 12 (*Fgf12*), a 600 Kb gene that controls sodium current kinetics at the axon hillock. A strong and transient epistatic interaction existed between the *Oprm1* and *Fgf12* loci during a short time window (45-75 min). The combination of a *B* haplotype at *Oprm1* with a *D* haplotype from DBA/2J at *Fgf12* was associated with unusually high activity. In a complementary study in heterogeneous stock rats, we demonstrated that *Oprm1* and *Fgf12* were co-expressed in one specific subtype of Drd1^{+} medium spiny neuron. A Bayesian network analysis supported an *Oprm1*-to-*Fgf12* network that involves a MAP kinase cascade that modulates *FGF12* phosphorylation and locomotor activation. *OPRM1* and *FGF12* networks in human GWAS data highlight enrichment of signals associated with substance use disorder. This study represents the first demonstration of a time-dependent epistatic interaction modulating drug response in mammals and the first linkage of *Fgf12* to opioid-induced behavior.

Introduction

Understanding the molecular genetics of opioids is crucial for treatment of opioid use disorder (OUD). Great progress has been made recently in genome-wide association studies (GWAS) of OUD. Genetic variants of several genes have reached genome-wide significance, such as *KCNC1*, *KCNC2* (Gelernter et al., 2014), *CNIH3* (Nelson et al., 2016), *RGMA* (Cheng et al., 2018), *KDM4A* (Sanchez-Roige et al., 2021), and *OPRM1* (Zhou et al., 2020). Recently, Deak and colleagues (2022) have identified an additional set of 19 independent risk loci for OUD.

Most of these variants explain a relatively small fraction of the heritability of OUD and require validation.

The most replicated gene among these studies is the opioid receptor gene *OPRM1* (Deak et al., 2022; Gaddis et al., 2022; Zhou et al., 2020), which encodes the μ opioid receptor (MOR).

Morphine, the prototypic MOR agonist, inhibits adenylyl cyclase and decreases the transmission of nociceptive information (Yam et al., 2018). Activation of MOR also increases dopaminergic neuronal transmission to the nucleus accumbens (NAc) by inhibiting GABAergic interneurons in the ventral tegmental area (VTA) (De Vries and Shippenberg, 2002). Coexpression of both MORs and dopamine D1 receptors (DRD1)—but not D2 receptors (DRD2)— is required for the initial locomotor response to morphine (Severino et al., 2020). MOR activation in striatal neurons is also a sufficient signal of opioid reward (Cui et al., 2014). However, the downstream molecular networks associated with *OPRM1* activation and signaling remain incompletely understood.

The lack of large and well phenotyped populations is a major impediment to further discovery of specific genes and mechanisms that modulate different phases of OUD (Berrettini, 2017). Compared to human GWAS, genetic mapping using model organisms requires a much smaller sample size. Phenotypes can be measured more accurately and studied mechanistically with better control over environmental variables. Large families of recombinant inbred strains (RI) are especially powerful for identifying genetic drivers responsible for trait variation, such as responses to opioids. These families are made by crossing two or more inbred strains, followed by intercrossing and inbreeding progeny for more than 20 generations (Williams et al., 2001).

The BXD RI family of mice was created by crossing C57BL/6J (B6) with DBA/2J (D2) (Ashbrook et al., 2021; Taylor et al., 1999, 1973). This family has been used to study the effects of alcohol and many psychoactive drugs (Belknap et al., 1993; Crabbe, 1998; Crabbe et al., 1983; Miner and Marley, 1995), along with numerous other molecular and complex traits.

The original data were described in Philip et al. (2010), who identified the *Oprm1* locus. Here, we significantly extended these analyses by using whole-genome sequence-based genetic maps (Ashbrook et al., 2021) and the GEMMA linear mixed model (LMM) (Zhou and Stephens, 2012) for mapping, which improves mapping power and controls for population structure better than previously used methods. In addition to *Oprm1*, our analysis identified a new morphine response locus on chromosome 16 (Chr 16). We exploited complementary rodent data sets—both whole brain proteomics and single-nuclei RNAseq—and identified a new candidate gene—fibroblast growth factor 12 (*Fgf12*). We found a strong and transient epistatic interaction between the *Oprm1* and *Fgf12* loci in a short time window after morphine injection.

The snRNA-seq data highlights a single subtype of *Drd1*-positive cell type in which *Oprm1* and *Fgf12* are coexpressed. We then created a probabilistic causal model formalizing a molecular scheme in which gene variants modulate key signaling molecules to control locomotion after morphine injection. Lastly, we integrated rodent data with comparable human gene expression to provide a better translational context for understanding the molecular mechanisms and cellular cascades that may underlying initial variation in human OUD responses.

Results

QTL mapping of morphine-induced locomotor responses

A total of 64 fully inbred strains from the BXD family (Ashbrook et al., 2021) were used. Each strain was represented by an average of six males and six females (Philip et al., 2010).

Locomotion was recorded for 180 min after an acute morphine injection, with movement data binned for each 15 min period. All data were generated by co-authors (PED, GM). Data for the 10th time bin (135–150 min) were lost. Variation in locomotor responses revealed a skewed distribution (Supplementary Figure 1). We therefore quantile normalized data (Supplementary Figure 2) for most analyses, although we note that linkage statistics are robust with respect to this transformation.

QTL linkage was computed using a subset of ~7,000 informative sequenced-based markers selected via linkage disequilibrium pruning and using the latest version of GEMMA v0.98.5 (Prins et al., *github.com/genetics-statistics/GEMMA*) as implemented in *Genenetwork.org*. The genome-wide –logP significance threshold (p <0.05), determined by 1,000 permutations, is approximately 3.77 for the BXD family. A list of genome-wide significant loci for both morphine-induced locomotion and naloxone-induced withdrawal was summarized in Table 1, with more details provided in Supplementary Table 1. We analyzed both sexes separately and jointly to identify potential sex-specific genetic modifiers of morphine response, because significant sex by strain interaction was detected in our prior analysis (Philip et al., 2010).

Throughout the first two hours after injection of morphine (0–135 min bins) we detected a single and highly significant locus on Chr 10 (Figure 1) with peak linkage that extends from about 5.7 to 8.9 Mb in males and from 8.9 to 9.6 Mb in females, and maximal –logP score of 10 and higher for males and 9.6 and higher for females (Figure 2) using quantile normalized locomotor data. This strong locus was reported by Philip et al. (2010). But we also now detect a strong second locus for locomotor activation on Chr 16 between 25 and 30 Mb, that only emerges 90 minutes after injection, and that reaches its temporal peak more than two hours after injection (Figure 3). Linkage is significant in both sexes but is several orders of magnitude stronger in females than males—linkages of 10.6 and 4.28, respectively.

Males and females display roughly similar patterns of linkage on both Chr 10 and Chr 16.

This is consistent with the generally strong positive sex correlations in morphine-induced locomotion responses across all 15-minute intervals. Correlation coefficients peak at about 0.84 to 0.88 from 15 to 75 minutes after injection—the phase during which morphine induces the steepest increase in locomotion—from about 29 to 71 m per 15 min bin (Figure 1c-d). This is also the interval that corresponds to the peak linkage in both sexes near *Oprm1*. Thereafter, correlations drop but are still generally above 0.70 through to 120 min. During the last hour correlations are lower—ranging from 0.57 to 0.68. This drop in correlation corresponds to the period during which effects of the *Fgf12* locus are strongest, and conversely, effects of the *Oprm1* locus are weakest. The distance traveled in the final interval (165 to 180 min) is down to a level slightly lower than that in the first interval—about 25 meters—and the final correlation between sexes is 0.68. This is the interval during which the *Fgf12* locus has a remarkably high linkage of 9.7 and 5.3 in females and males, respectively. In contrast, at this late stage *Oprm1* has linkage below 2.5 in both sexes.

Candidate gene identification for morphine-induced locomotor response

The mu 1 opioid receptor protein (MOR or OPRM1) is expressed in multiple brain regions and is involved in opioid-induced reward and locomotor response (Contet et al., 2004). In mice the very large *Oprm1* gene is on Chr 10 between 6.76 and 7.04 Mb, just proximal to the linkage peak (Figure 2c-d, GRCm38 assembly). In the BXD family there are over 40 known SNPs, indels, and larger variants segregating in this gene locus, but to the best of our knowledge none alter protein sequence. Given its location just proximal to the QTL peak, its large size, and the high level of

				Locus position (Mb, GRC38)							
Locus	Sex‡	Peak –logP*	Chr	Prox	Peak	Distal	1.5 –logP Interval	Add. Effect $	GN short phenotype description	Time Period (min)	GN BXD Trait
Mor1a	F	4.42	1	72.3	77.6	78.4	6.1	-0.42	Morphine-induced locomotion, distance traveled	0-15	11583
Nalx1a	MF	3.96	1	124.0	128.5	141.8	17.9	-0.43	Naloxone-induced withdrawal, salivation	NA	11875
Nalx1b	MF	4.14	1	163.3	167.2	168.2	4.8	-0.44	Naloxone-induced withdrawal, salivation	NA	11875
Mor1b	F	4.32	1	173.4	173.5	176.2	2.8	-0.38	Morphine-induced locomotion, distance traveled	150-165	11584
Mor4a	M	4.06	4	19.7	21.7	33.1	13.4	-0.39	Morphine-induced locomotion, distance traveled	45-60	11331
Mor5a	F	5.01	5	9.8	9.8	13.4	3.5	0.52	Morphine-induced locomotion, distance traveled	105-120	11581
Mor5b	F	3.86	5	76.1	82.2	90.4	14.2	0.41	Morphine-induced locomotion, distance traveled	30-45	11587
Nalx6a	MF / F	4.69	6	112.1	116.9	122.8	10.7	-0.42	Naloxone-induced withdrawal, horizontal activity	0-15	11871
Mor7a &	M / F	5.28	7	96.0	96.8	97.5	1.5	-0.44	Morphine-induced locomotion, distance traveled	0-15	11326
Mor9a	F	3.90	9	83.1	83.9	86.1	3.0	0.45	Morphine-induced locomotion, distance traveled	120-135	11582
Mor10a †	M / F	10.53	10	5.6	5.6	9.6	4.0	-0.59	Morphine-induced locomotion, distance traveled	30-45	11330
Nalx12a	MF / F	4.91	12	16.6	27.6	28.5	11.9	0.46	Naloxone-induced withdrawal, horizontal activity	0-15	11871
Mor12a	F	4.03	12	69.6	70.8	74.7	5.2	-0.42	Morphine-induced locomotion, distance traveled	0-15	11583
Mor12b	F	5.71	12	98.6	99.6	102.5	3.9	-0.44	Morphine-induced locomotion, distance traveled	30-45	11587
Nalx14a	M	4.00	14	49.1	52.1	61.2	12.1	-0.41	Naloxone-induced withdrawal, number of jumps	NA	11336
Nalx14b	MF	4.36	14	118.4	118.5	119.4	1.0	-0.25	Naloxone-induced withdrawal, horizontal activity	0-15	11871
Mor16a †	F / M	10.56	16	27.0	27.5	29.9	2.8	-0.61	Morphine-induced locomotion, distance traveled	165-180	11585
Nalx16b	MF	4.02	16	57.5	59.7	62.2	4.6	0.42	Naloxone-induced withdrawal, salivation	NA	11875

† Significant for morphine and naloxone treatments; best candidate for Mora10a is *Oprm1*; best for Mor16a is *Fgf12*.
‡ MF = male and female joint mapping. M / F = significant in both sexes but –logP value applies to first entry.
* –log*P* values given for quantile normalized traits but verified on other scales. Values are genome-wide $P \leq .05$ at ≥3.80.
$ Positive additive effects mean higher trait values linked to *D* genotypes. Negative values linked to high *B* values.
& Strong candidate gene for *Mor7a* is *Tenm4*.

Table 1. **Genome-Wide Significant Loci for Morphine-Induced Locomotion or Naloxone-Induced Withdrawal**

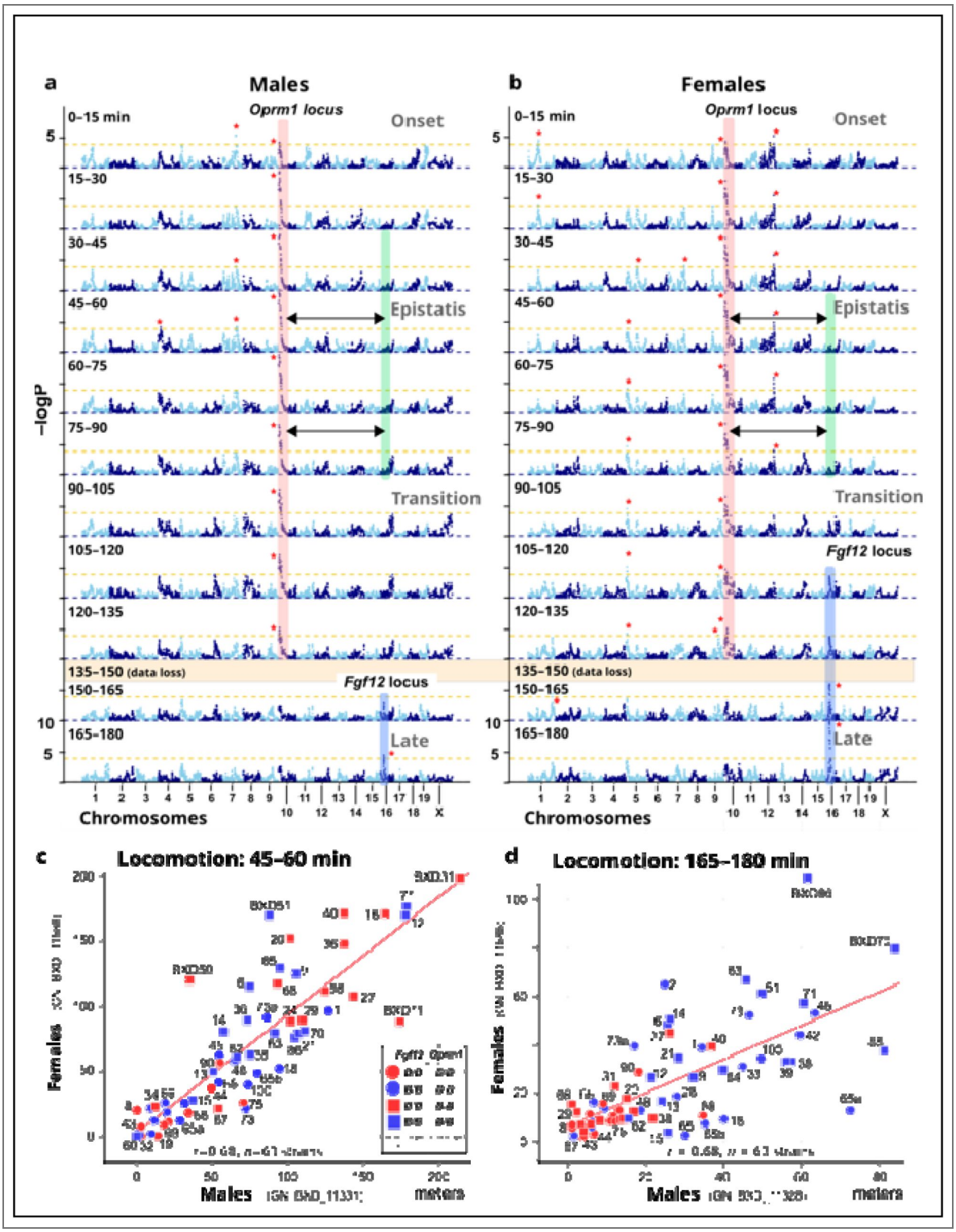

Figure 1. Time series of QTLs for morphine-induced locomotor response.

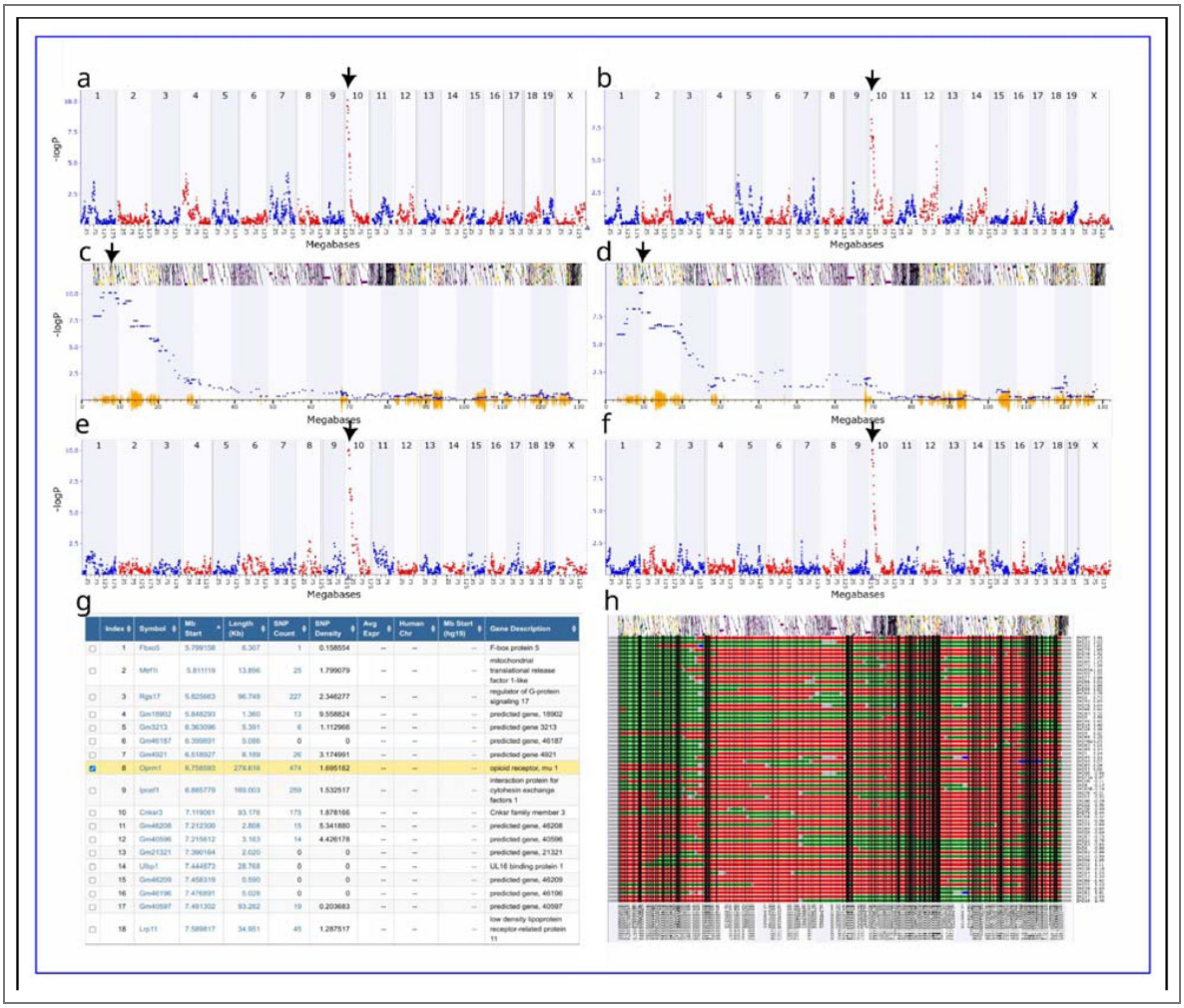

Figure 2. QTLs of morphine-induced locomotion between 45–60 min on Chr 10.

(a) QTL for males with a peak –logP of 10.06 (n = 63 strains). (b) QTL for females with a peak –logP of 9.60 (n = 64 strains). (c) Zoomed-in view of QTL in males. (d) Zoomed-in view of QTL in females. (e) Cis-eQTL for Oprm1 in the NAc of the BXDs, with a peak –logP of 10.01 (n = 34 strains). (f) Cis-eQTL for Oprm1 in the hippocampus of the BXDs, with a peak –logP 9.7 (n = 67 strains) on Chr 10 at 5.6Mb. (g) Oprm1 neighborhood in BXD family with SNP densities. (h) Haplotype map of the eQTL region. The "B" of BXD is the mother, and "D" is the father. GEMMA with LOCO was used for all association mapping.

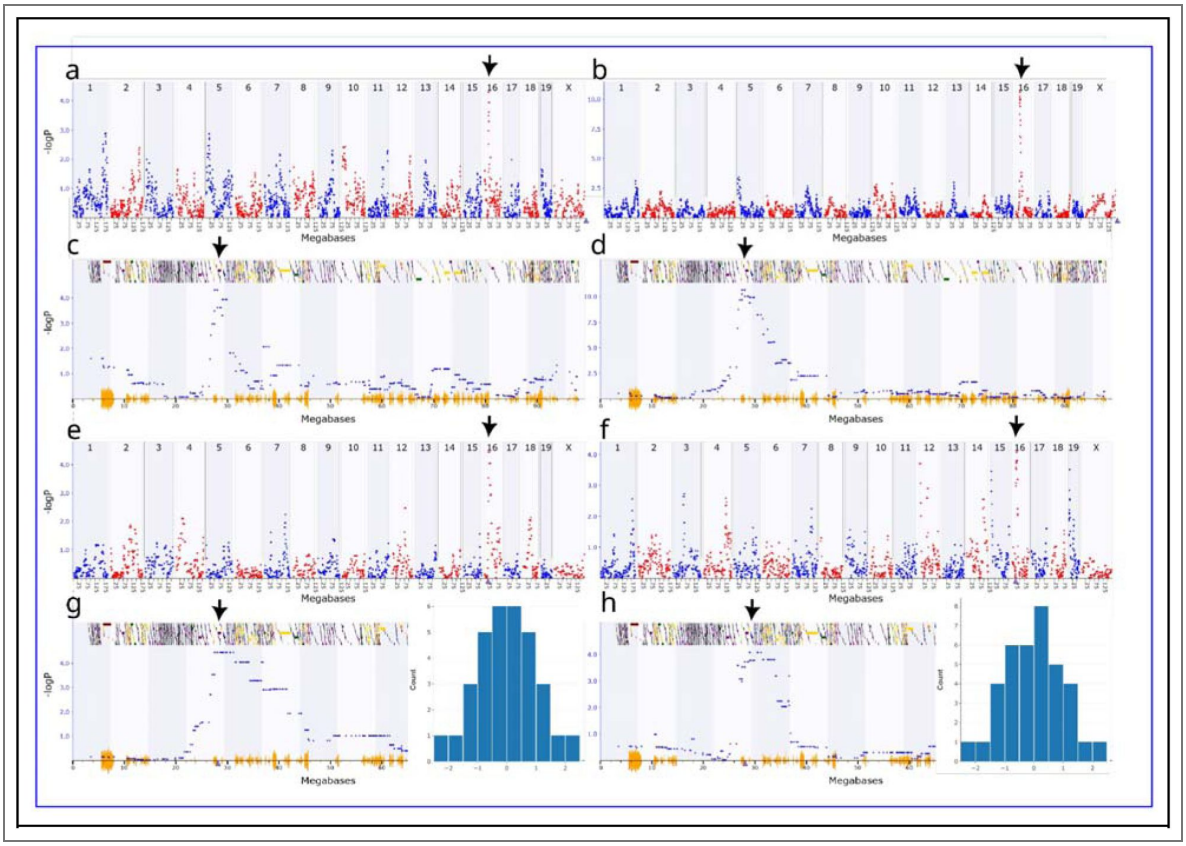

Figure 3. QTLs of morphine-induced locomotion between 165–180 min on Chr 16.

(a) QTL in males with a peak –logP of 4.28 (n = 63 strains). (b) QTL for females with a peak –logP of 10.56 (n = 64 strains). (c) Zoomed-in view of the QTL in males. (d) Zoomed-in view of the QTL in females. (e) Cis-eQTL in the striatum of the BXDs, with a peak –logP of 4.43. (f) Cis-eQTL in the VTA of the BXDs, with a peak –logP of 4.06. (g) Histogram of the normalized expression of Fgf12 in striatum and zoomed in view of the QTL region. (h) Histogram of the normalized expression of Fgf12 in VTA and zoomed in view of the QTL region. GEMMA with LOCO was used for all association mapping.

genetic variation, *Oprm1* is an uncontroversial candidate for differences in acute morphine locomotor activation (Table 2). But there is some additional support—expression of *Oprm1* mRNA has been quantified in many brain regions across the BXD family, and variants in and around this gene clearly modulate its expression most strongly in nucleus accumbens (NAc) and hippocampus (cis-eQTLs with –logP values >7.0, see examples in Figure 2e,f).

Variation in the expression levels of *Oprm1* from the *B* and *D* haplotypes could contribute causally to the Chr 10 locus. Of functional importance, the *D* allele has roughly 50% higher expression in both NAc (Figure 2e) and hippocampus (Figure 2f), an interesting observation given that BXD strains that inherit the *B* allele tend to have a much stronger initial locomotor response.

We restricted our analysis of candidate genes for the novel Chr 16 locus to a 1.5 –logP confidence interval (corresponding to a 95% confidence interval) extending from 27 to 29 Mb (Figure 1). This small region contains only five protein-coding genes and one gene model (*Gm10823*) in the following proximal-distal order: *Ostn*, *Uts2d*, *Ccdc50*, *Gm10823*, *Fgf12*, and *Mb21d2* (Figure 4). *Fgf12*, previously known as *Fhf1*, is the largest protein-coding gene in this interval (~600 Kb), with a promoter located close to *Mb21d2* (Figures 3c–d, Figure 4). This is also the strongest biological candidate gene (Table 2), and is already known to interact with the C-terminal region of three sodium channel proteins— SCN9A (Wildburger et al., 2015), SCN8A (Liu et al., 2003), and SCN2A (Wildburger et al., 2015). *Fgf12* encodes a protein that is a member of the fibroblast growth factor (FGF) family. FGFs are involved in response to alcohol (Even-Chen et al., 2017) and morphine (Flores et al., 2010) in key brain reward regions.

The majority of the *Fgf12* gene is situated in a region that is almost identical-by-descent between the *B* and *D* parental haplotypes. This is highlighted in Figure 4 as the very low SNP density. There are 12 known non-coding variants between *B* and *D* haplotypes, and no known coding variants, however, there are very significant cis-acting expression QTLs associated with *Fgf12* expression differences in the striatum (Figure 3e,g, –logP of 4.4) and the ventral tegmental area (Figure 3f, h –logP of 4.1). The *B* allele is associated with expression that is as much as 60% higher than that of the *D* allele. We identified no coding variants for the other genes in this interval, and *Fgf12* showed the most robust cis-eQTL evidence.

An epistatic interaction between *Oprm1* and *Fgf12* loci modulates locomotor response to morphine

We detect large additive effects for the locomotor responses to morphine near *Oprm1* at early time points (0–90 min) and near to *Fgf12* at late time points (+90 min). We tested for a possible epistatic interaction between these distinct loci and discovered a strong but transient interaction in both sexes (Figure 5). The epistasis is strongest in the 45–60 min period—precisely at the midpoint between the early and additive *Oprm1* effect and the late and additive *Fgf12* effect (Fig 8c-g, e.g., male trait BXD_11331). Those BXDs that inherit the *B* haplotype of *Oprm1* (defined as rs29339674, 6.7 Mb) as well as the *D* haplotype of the *Fgf12* locus (defined as rs4169220 at 31.6 Mb) have unexpectedly high levels of locomotion compared to all of the other two-locus combinations (Figure 5, Supplementary Figure 3). The –logP value of the epistatic component is in the range of 2.5-4.8 (MF = trait BXD_11845, –logP = 4.2; F trait = BXD_11588, –logP = 4.8; M trait = BXD_11331, –logP = 2.5) and is significant at $p < 0.05$. The full model that includes this interaction term, as well as both additive effects at *Oprm1* and at *Fgf12* has a remarkably high –logP value of 11.9-13.2 (MF = 13.2, F = 11.9, M = 12.0). This epistatic interaction is preserved as the time window moves forward. For example, maps of the 60–75 min interval (trait BXD_18846) has an epistatic effect with a –logP of 3.0; an additive effect near *Oprm1* with a –logP of 8.2; and an additive effect at *Fgf12* of merely 0.14. The full model in this interval still has a very high cumulative –logP of 11.4. By 75–90 minutes (trait BXD_18847) the interaction effect has dropped to a –logP of 2.2 and the model has a cumulative –logP of 9.40. In marked contrast, over the two intervals from 90 *to* 120 minutes we do not detect significant epistasis. At best, the interaction –logP is only in the range of 1.5–2.0. In the 120–135 and 150–165 minute intervals the originally powerful *Oprm1* additive effect has faded to 2.74 and 1.15, respectively. There is no detectable interaction with the *Fgf12* locus. However, the purely additive effect at *Fgf12* is now much stronger and is detectable for the first time as an

Table 2. **List of Candidate Genes**

Candidate Gene	Chr	Start (Mb)	Stop (Mb)	Male Trait ID	Female Trait ID	Phenotype
Tenm4	7	96	97.5	BXD_11326	BXD_11572	Locomotoin 0-15min after morphine injection
Oprm1	10	5.6	9.6	BXD_11331	BXD_11588	Locomotion 45-60min after morphine injection
Oprm1	10	5.6	9.6	BXD_11339	BXD_11596	Differences in locomotion before vs. after injection
Slc7a7/slc7a8	14	49.1	61.2	BXD_11336	BXD_11850	Number of jumps After naloxone-induced withdrawal
Fgf12	16	27.0	29.9	BXD_11328	BXD_11585	Locomotion 165-180min after morphine injection
Fgf12	16	27.0	29.9	BXD_11339	BXD_11596	Differences in locomotion before vs. after injection

Potential candidate genes in QTL regions that were further investigated in this study are provided. For details on any given trait, please visit the corresponding GN website by embedding the trait ID in the URL such as https://genenetwork.org/show_trait?trait_id=11331&dataset=BXDPublish (for trait BXD_11331, Morphine response (50 mg/kg ip), locomotion (open field) from 45-60 min after injection in an activity chamber for males [cm]).

Figure 4. **Chr 16 locus at 165-180 min after morphine injection.**

(a) Zoomed in view of the Chr 16 locus, from 26-29 Mb, showing individual SNPs (blue dots) and genes (purple horizontal lines) in the region. (b) A screenshot of GeneNetwork showing SNPs that inhabit this region. Almost all B vs D SNPs (orange hash along x-axis) are restricted to two regions.

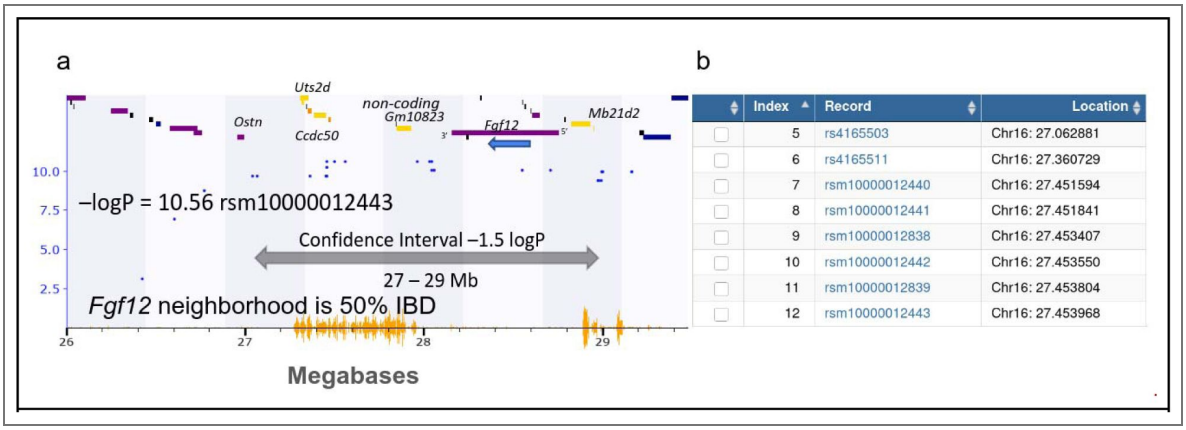

independent additive effect with –logP values of 2.1 and 4.2, respectively. Finally, in the last interval—165–180 minutes (trait BXD_11585)—we detect no linkage to the *Oprm1* locus, or any epistasis, but we again pick up a highly significant additive effect at the *Fgf12* locus with a peak –logP that is 4.9.

Cell-type-specific co-expression of *Oprm1* and *Fgf12* in the rat nucleus accumbens core

To further examine whether *Oprm1* and *Fgf12* were co-expressed in the same cells of the NAc, we performed snRNA-seq using a droplet-based approach (10X Genomics). Nuclei were isolated from microdissected NAc cores obtained from two female heterogeneous stock (HS) rats (Carrette et al., 2021). The NAc was chosen due to its central role in opioid reward and the observed strain differences in morphine-induced locomotion (Velásquez et al., 2019). After filtering out low-quality nuclei and potential doublets, a total of 4,495 high-quality nuclei transcriptomes remained with a median number of 3,363 transcripts (unique molecular identifiers) and 1,861 genes detected per nucleus. We then performed SCT transformation (Hafemeister and Satija, 2019), dimensional reduction, and clustering using Seurat (Stuart et al., 2019) and identified 17 cell-type clusters (Figure 6a).

We annotated the cell clusters based on the expression level of established marker genes of the major cell types: neurons (*Snap25*, *Syt1*), excitatory neurons (*Slc17a7*), inhibitory neurons (*Gad1*), dopaminergic neurons (*Ppp1r1b, Foxp2, Blc11b*), oligodendrocytes (*Mbp*), oligodendrocyte precursor cells (*Pdgfra*), astrocytes (*Aqp4*), and microglia (*Arhgap15*). In addition, we identified 7 subtypes of dopaminergic-receptor neurons. We used expression of *Drd1* and *Tac1* to define D1-type medium spiny neurons (D1-MSNs). The expression of *Drd2* and *Penk* was used to define D2-type medium spiny neurons (D2-MSNs) (Figure 6b, n = 1,768 MSNs total, see Supplementary Figure 4f). MSNs represented the majority (91.8%) of neuronal cells, as expected by previous knowledge of the NAc cellular composition.

Oprm1 was uniquely expressed in the D1-MSN-3 subtype, while *Fgf12* was expressed across all cell populations (Figure 6c,d). We then performed Pearson's correlation analysis to test the idea that the epistatic interaction between *Oprm1* and *Fgf12* is mediated by a specific cell type. While a weak but significant positive correlation (r = 0.08, p = 1.8e-8) between the expression of *Oprm1* and *Fgf12* (Figure 6e) were detected when all cell were included, a much stronger correlation (r = 0.35, p = 6.1e-8, Figure 6f) was found in D1-MSN-3 cells. In contrast, D1-MSN-2 had a significant weak negative correlation (r = –0.12, p = 0.02, Figure 6g). In conclusion, D1-MSN-3 is the only cell cluster expressing a high level of *Oprm1* in rat NAc, in which the expression levels of *Oprm1* and *Fgf12* are significantly and positively correlated.

Constructing and testing Bayesian networks

We hypothesize that genetic variants in the Chr 10 and Chr 16 QTL regions are driving differential expression of *Oprm1* and *Fgf12* in the BXD family and thereby modulating morphine-induced locomotor responses. We used the literature to guide our selection of mediators acting between *Oprm1* and *Fgf12* (Bhushan et al., 2017; Buchsbaum et al., 2002). For example, *FGF12* (Sochacka et al., 2020) and *MAPK8IP2* are linked to a few sodium channel components—SCN2A (Nav1.2) and SCN8A (Nav1.6)(Schoorlemmer and Goldfarb, 2001; Seiffert et al., 2022)—as part of a membrane-associated scaffold concentrated at the axon hillock. The *MAPK8IP2* scaffold protein is thought to modulate JUN amino-terminal kinase signaling, and also interacts with and controls the activity of MAPK8/JNK1 and MAP2K7/MKK7 (O'Leary et al., 2016).

We tested *Scn2a, Scn8a, Map3k11*, *Map3k12*, and *Mapk8ip2* as candidate mediators of the *Oprm1* and *Fgf12* loci and variation in locomotor activity. Expression levels of these transcripts in striatum, VTA, and NAc of BXD strains were passed from GeneNetwork into the Bayesian Network (BN) Webserver (Ziebarth and Cui, 2017) to define the most probable network structure. We constrained the nodes into four tiers: Tier 1 contains the two loci as instrumental variables; tier 2

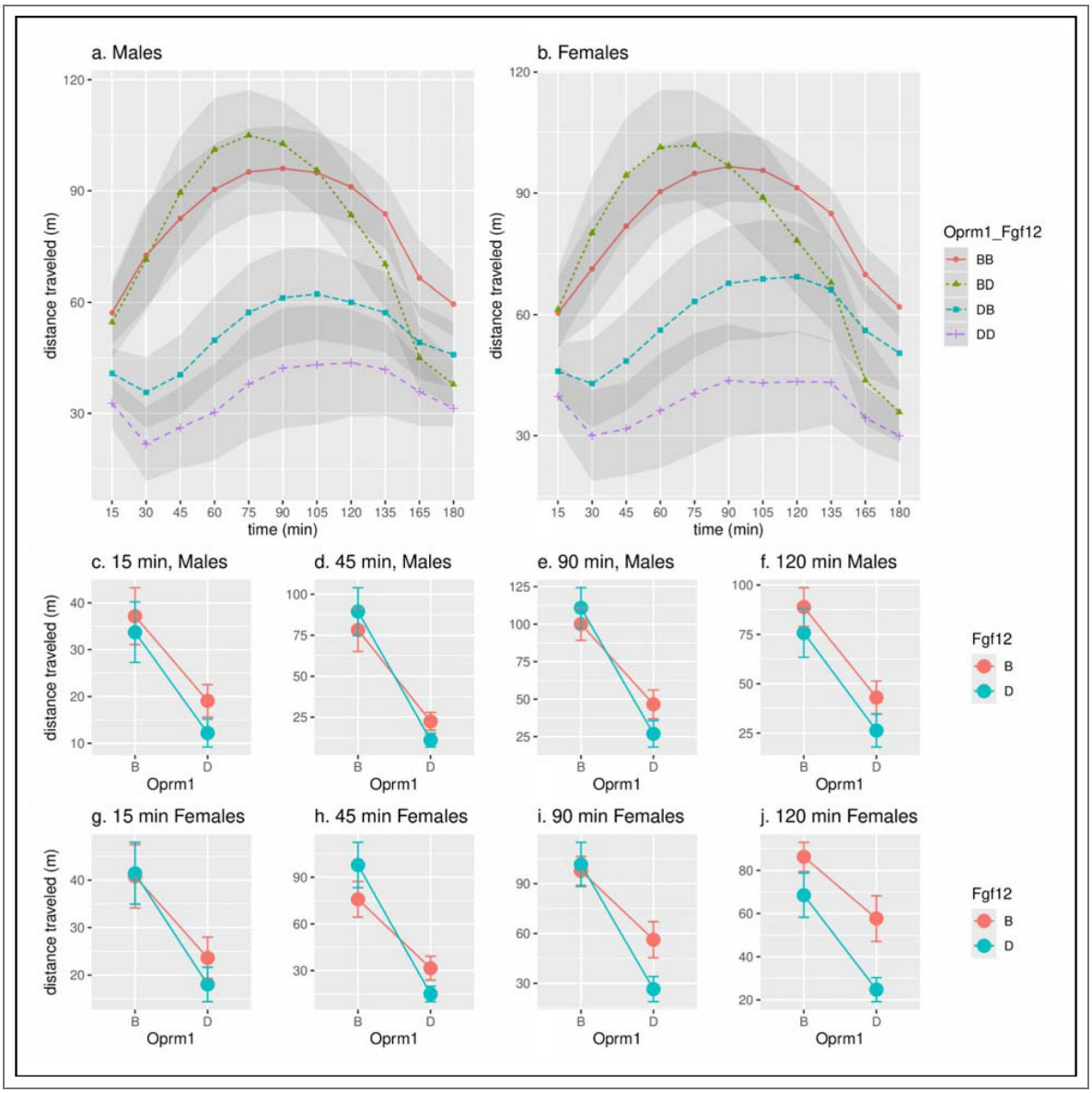

Figure 5. Epistatic Interaction Among Genotype Combinations.

(a) Males and (b) females with different combinations of the "B" (i.e., B/B) or "D" (i.e. D/D) genotypes yield different distances traveled after morphine injection over 120 mins. Distance traveled (m) between the two genotypes for each loci is shown for each timepoint in (c-f) males and (g-j) females.

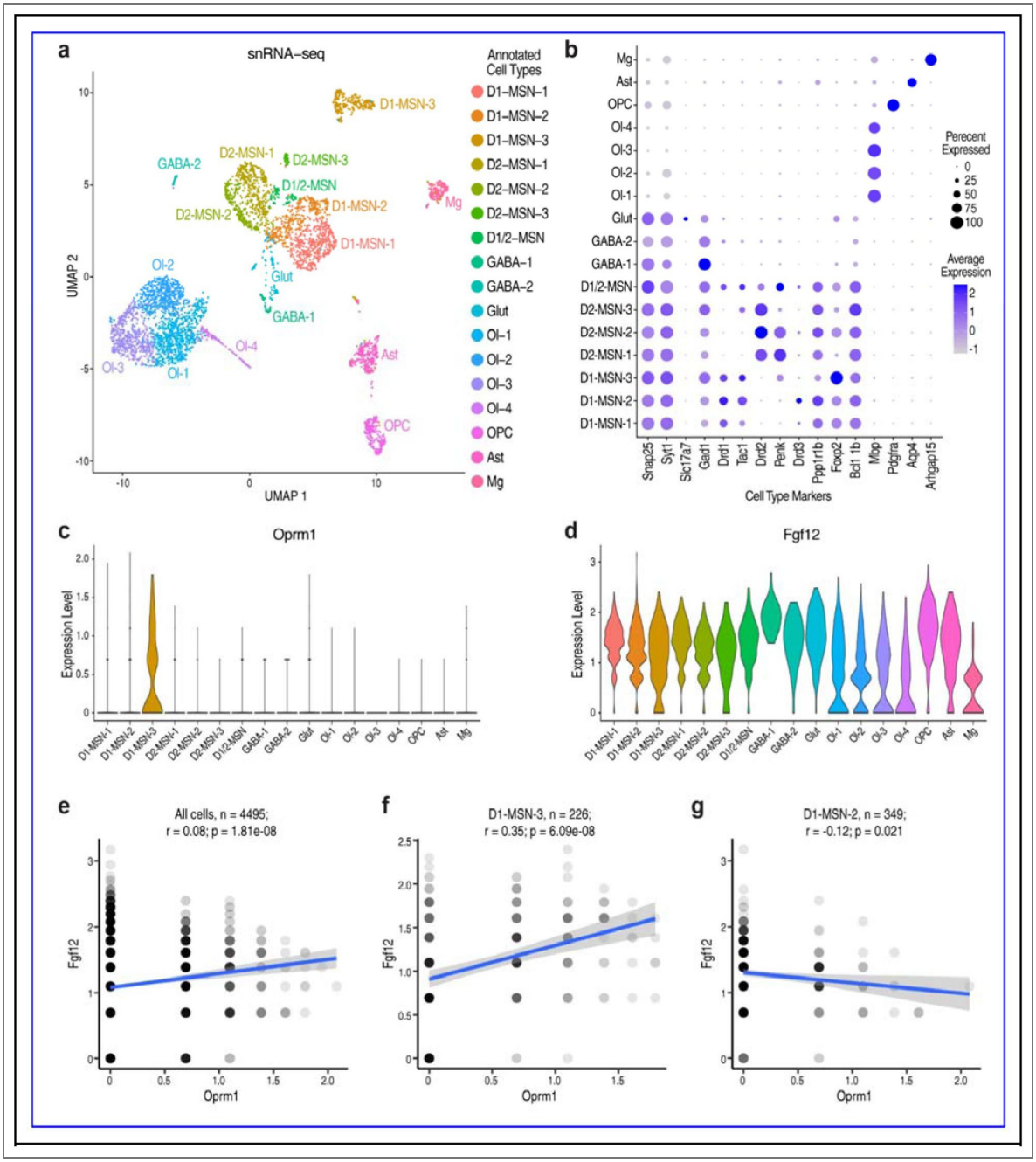

Figure 6. Oprm1 and Fgf12 are positively correlated in rat NAc suggested by snRNA-seq.

(a) UMAP visualization of cell clusters from 4495 nuclei from rat nucleus accumbens core. (b) Dot plot showing the expression level of cell type marker genes in cell clusters. The shade of dots denotes normalized and scaled average expression and the size of dots denotes the percentage of cells expressing the gene in each cell cluster. (c-d) Violin plots indicating the normalized and scaled expression level of Oprm1 (c) and Fgf12 (d) across cell clusters. (e-g) Scatter plots showing the correlation relationship between Oprm1

contains expression estimates of the two prime candidate genes, *Oprm1* and *Fgf12*; tier 3 contains the sodium channels and MAP kinases that potentially mediate both additive and epistatic effects on locomotion; and tier 4 contains the locomotor outcomes expressed in four time-series bins.

The most strongly supported model (Figure 7) recapitulated the cis-eQTL results by indicating that the Chr 10 and Chr 16 loci control the expression of *Oprm1* and *Fgf12* mRNA.

This model also supports the causal role of *Oprm1* and its downstream MAP kinases on locomotor response during the first 120 minutes after injection. In contrast, the last 45 minutes are dominated by a direct *Fgf12* effect. Further, *Oprm1* and *Fgf12* directly modulate *Map3k11*, which in turn modulates *Mapk8ip2* and *Map3k12* mRNA expression and regulate locomotion from 0 to 75 min. Further, Mapk8ip2 is embedded in this network with multiple connections.

This Bayesian network aligns well with whole-brain proteomics data (supplementary figure 6). In agreement with the mRNA data, *Oprm1* and *Fgf12* are expressed with opposite polarities, in which the *B* allele is associated with high expression of *Oprm1* and low expression of *Fgf12* and vice versa for the *D* allele. The three MAP kinases are also expressed in higher levels in animals that inherit *B* alleles than *D* alleles.

QTL mapping of naloxone-induced withdrawal responses

Once the locomotion test was completed (180 min after the morphine injection), naloxone was injected (30 mg/kg in isotonic saline at a volume of 10 ml/kg) to induce a morphine withdrawal response (Philip et al., 2010). Locomotion and other behavioral measurements were taken for both males and females. QTL analysis of these traits were not included in Philip et al. (2010). There are an impressive 16 genome-wide significant QTLs among 5 naloxone-induced withdrawal behavioral responses (Figure 8, Supplementary Table 1).

Figure 8c-d displays the differences in locomotion before and after naloxone injection, with a QTL peak on Chr 10 and 16 that overlap the morphine locomotor QTLs in Figures 2 and 3 and that are likely to correspond to variants in or near to *Oprm1* and *Fgf12*. Our results show that the genotype effect on locomotion was similar before and after naloxone injection (Supplementary Figure 7). We evaluated the biological function of naloxone candidate genes using GeneCup (Gunturkun et al., 2022). Candidates for the locus on Chr 14 for naloxone-induced jumps include *Slc7a7* and *Slc7a8* (Table 2). Both are transmembrane amino acid transporter proteins (Hu et al., 2020) that dimerize with *SLC3A2(*Hurkmans et al., 2022*;* Torrents et al., 1999, 1998*)*. Of relevance, *SLC7A8* (LAT2) is an L-DOPA transporter(Crocco et al., 2024).

Integrating murine data with human GWAS results

There is strong support for *OPRM1* in human OUD GWAS. *OPRM1* variant rs1799971 has been associated with OUD in several studies [e.g., $p = 8 \times 10^{-10}$ in Zhou et. al. (2020), $p = 2 \times 10^{-8}$ in Hatoum et. al. (2022a), and $p = 4.92 \times 10^{-9}$, OR = 1.046, in Deek et. al. (2022)]. A human GWAS of opioid cessation reported linkage to the FGF signaling pathway in which the effect of *FGF12* was nominally significant ($p = 0.0015$, odd ratio = 1.24) (Cox et al., 2020). In gene-based analyses of OUD by Deak et al. (2022), there was a nominally significant signal for *FGF12* ($p = 0.006$), with the top FGF12 SNP rs1553460 also reached nominal significance (OR = 1.015, p = 0.021).

Considering the epistatic interaction between *OPRM1* and *FGF12* and the complexity of human genetic signals (many genes of small effects) it is possible that these two genes function in a network that contains many other genes. We thus developed a list of 500 genes that overlap with *FGF12* and *OPRM1* in the GTEx sample (GTEx Consortium, 2013) (GTEx v8). We then examined whether there is enrichment of members of this network using MAGMA (de Leeuw et al., 2015) in the GWAS by Zhou et al.(2020). Our initial analysis was performed for NAc, putamen, caudate, and adipose tissue for the *FGF12* lists (the latter as a negative control).

For OUD, no significant enrichment was observed for the original 500-gene lists, likely due to the lists' large size and the limited statistical power of the SUD GWAS. In the GWAS conducted by Deak et al. (2022), where *FGF12* was nominally significant, we found nominally significant enrichment in two of the brain regions, putamen and caudate. Given the low power of this dataset

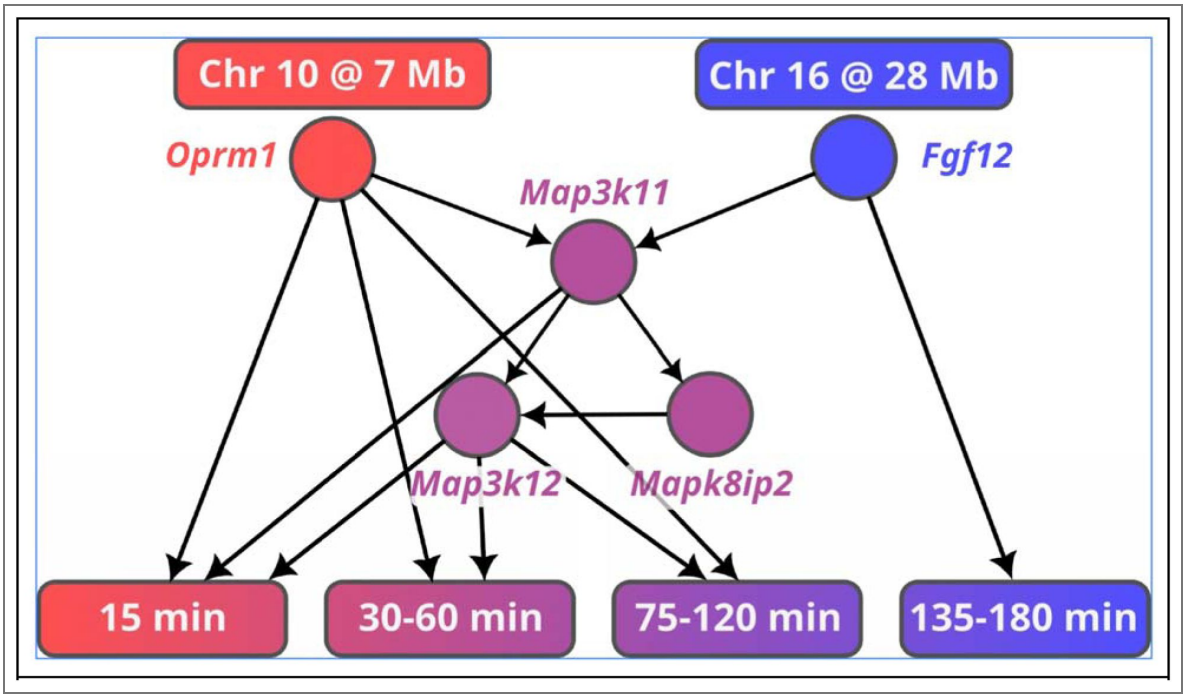

Figure 7. Modeling the mechanistic interactions between genetic variants and phenotypes using Bayesian network.

This network illustrates the relationship between genetic variants in the Chr 10 and Chr 16 QTL regions and the differential expression of candidate genes Oprm1 and Fgf12 in the BXD family. Additional gene expression data of MAP kinases were retrieved from *Genenetwork.org*. Morphine induced locomotion responses at different time bins are also included in the network. This causal hypothesis was developed using the Bayesian network framework available in Genenetwork, where the arrow is indicative of the direction of the causal relationship. Additional genes included in the input of the network construction but had no connection to the final network were excluded in the illustration.

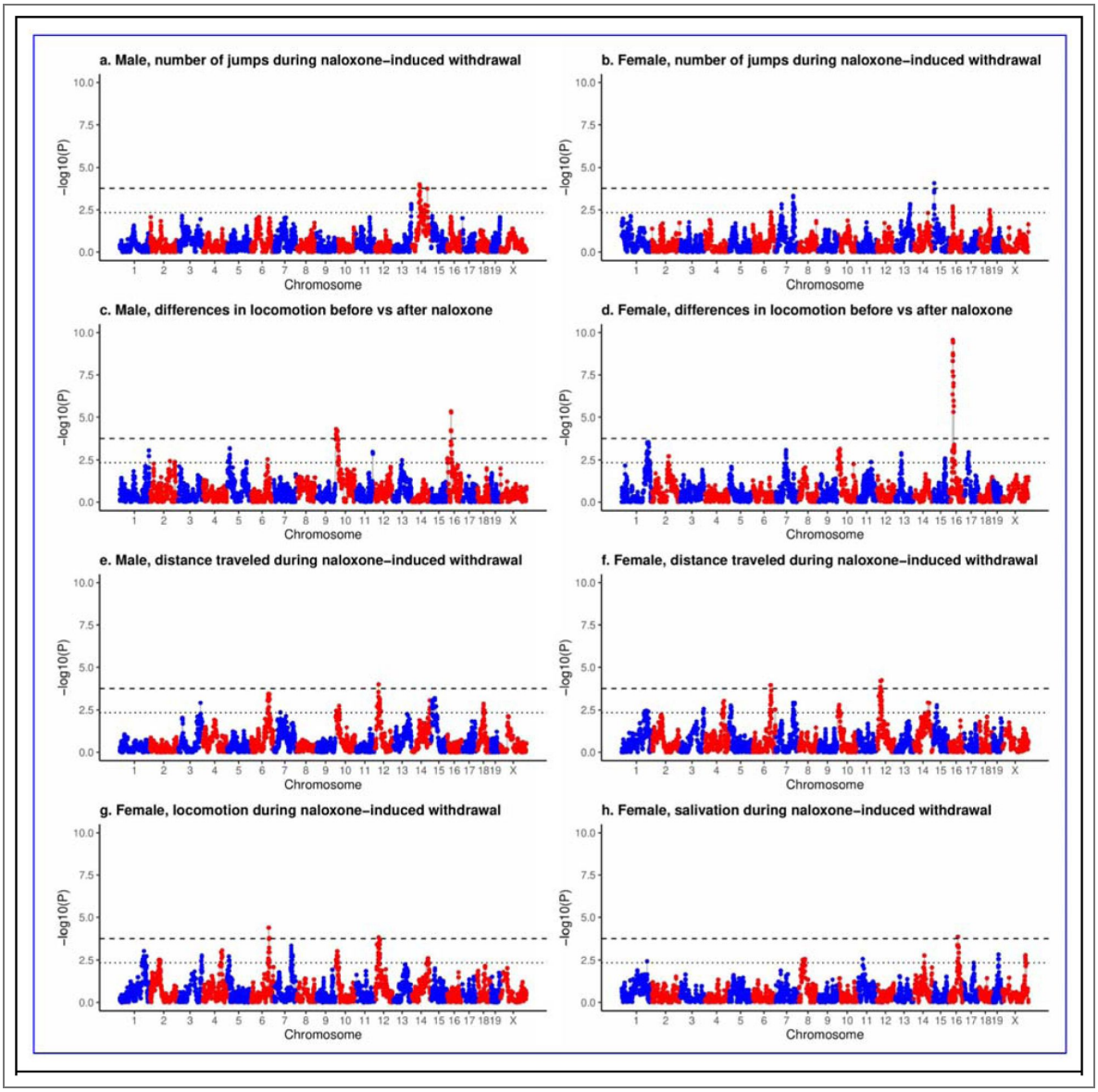

Figure 8. QTLs for naloxone-induced morphine withdrawal responses in males and female BXD mice.

Behavior data were quantile normalized and mapped against WGS-based genotypes using GEMMA in *Genenetwork.org*. (a) Number of jumps 15 minutes after naloxone injection in males. (b) Number of jumps 15 minutes after naloxone injection in females. (c) Change in locomotion measured by the last 15 min of morphine locomotion response minus the first 15 min after naloxone injection in males, with a peak on Chr 10 and a peak on Chr 16 (d) Change in locomotion measured by the last 15 min of morphine locomotion response minus the first 15 min after naloxone injection in females, with a peak on Chr 16. (e) Horizontal activity (distance traveled) 0–15 min after naloxone injection for males. (f) Horizontal activity (distance traveled) 0–15 min after naloxone injection for females, with a peak on Chr 6, and a peak on Chr 12. (g) Number of beam breaks in an open field 0–15 min after naloxone injection in females, with a peak on Chr 6 and a peak on Chr 12. (h) Salivation level in females. Dashed lines: genome wide significance threshold. Dotted lines: threshold for suggestive significance.

and the broad initial gene list, we refined our analysis to focus on genes specifically correlated with *OPRM1* and *FGF12* in relevant tissues (see Methods). No enrichment was observed for the gene network in the OUD GWAS (p = 0.493). However, this refined approach revealed nominal enrichment (p = 0.038) for the addiction risk factor (Hatoum et al., 2022b).

Discussion

We analyzed time-dependent behavioral responses to morphine and naloxone collected from the BXD family of mice (Philip et al., 2010) using WGS-based genetic markers and linear mixed models. We discovered a novel association on a Chr 16 locus that overlaps *Fgf12* in both sexes, in addition to confirming an association between locomotor response and a region on Chr 10 that overlaps *Oprm1*. Further, these two loci had a significant but transient epistatic interaction between 45–90 min after morphine injection. According to our transcriptomic data from NAc in rats, *Oprm1* and *Fgf12* are colocalized in a specific subtype of D1-MSN and their expression levels are positively correlated. Analysis of both *OPRM1* and *FGF12* in human GWAS data demonstrated an enrichment of signals associated with SUD phenotypes, and a modest corroboration of variants in the *FGF12* locus on Chr 3q28.

Additive effect of the *Oprm1* locus

The proximal Chr10 locus associated with early phase locomotor response to morphine contains the *Oprm1* gene. This locus has been associated with the antinociceptive effect of morphine (Bergeson et al., 2001). *Oprm1* encodes the primary receptor responsible for morphine-induced locomotor response (Severino et al., 2020; Smith et al., 2009), and is also responsible for its addiction liability (Ballester et al., 2022; Zhang et al., 2020). Notably, the *Oprm1* mRNA cis-eQTL in the NAc and hippocampus precisely overlaps with the *Mor10a* QTL interval (Figure 2e, 2f), providing strong secondary evidence for *Oprm1* as the causal gene.

Morphine-induced locomotion was affected by *Oprm1* variants (Popova et al., 2019). For example, in the *Oprm1* A112G knock-in mouse, morphine-induced hyperactivity was blunted (Mague et al., 2009). Further, the effect of MOR on locomotion depends on the neuronal cell types involved. For example, when MOR was deleted from D1 neurons, mice had hypolocomotion in response to opioids. By contrast, when MOR was deleted from A2a (adenosine A2a receptor-expressing) neurons, mice displayed increased movement in response to opioids (Severino et al., 2020). These data indicate that *Oprm1* is a strong candidate gene for the Chr 10 locus associated with morphine-induced locomotion response.

BXDs with the *D* allele at the *Oprm1* locus were less sensitive to a 50 mg/kg dose of morphine (Figure 6). The locomotion data demonstrate a blunted motor activity response similar to what was seen in low doses of morphine (5 to 10 mg/kg) (Mori et al., 2004), while BXDs with the *B* allele demonstrate higher sensitivity at the same dose; strains with the *B* allele had an initial biphasic increase in motor activity followed by a drop. This suggests that the *B* allele of *Oprm1* is associated with greater sensitivity or locomotion activity. These data match the differences between the parents of the BXD family. The locomotor response to morphine in C57BL/6J is more pronounced and lasts longer compared to that of DBA/2J (Murphy et al., 2001). This dimorphism may be linked to differences in morphine-induced dopamine release in the NAc in C57BL/6J than in DBA/2J mice (Murphy et al., 2001).

Additive effect of the *Fgf12* locus

The association between the Chr 16 locus (Figure 1 a,b) and morphine-induced locomotion 150–180 minutes after injection is a novel finding, as is the detection of a time-delimited epistatic interaction of the Chr 16 locus with the *Oprm1* locus. The use of a high-density WGS-based marker set and the LMM (GEMMA) allowed us to detect this and other novel loci not previously detected. Of all positional candidate genes in the Chr 16 locus (Figure 4), *Fgf12* was the most biologically relevant and was supported by strong cis-eQTL in striatum and VTA (Figure 3 e,f). Studies have implicated members of the FGF family, such as *Fgf2* (Even-Chen and Barak, 2019a), FGF receptor 1 (Even-Chen and Barak, 2019b), and FGF receptor 2 (Blackwood et al., 2019) in substance use.

It has recently been demonstrated that administration of an *Fgf21* analog in non-human primates decreased alcohol consumption by 50% via an amygdala-striatal circuit (Flippo et al., 2022). Unlike these secreted FGFs, *Fgf12* is an intracellular protein that serves as a cofactor for voltage-gated sodium channels and other molecules and is involved in intracellular signaling events (Schoorlemmer and Goldfarb, 2001). While the full spectrum of its function remains unknown, *Fgf12* has demonstrated a role in locomotion. For example, mice with a null mutation of *Fgf12* have ataxia (Goldfarb et al., 2007). Elevated stress responses have been associated with a reduction in *Fgf12* expression in the prefrontal cortex in rats (McCreary et al., 2016). *FGF12* expression is also elevated in the anterior cingulate cortex of patients with major depressive disorder (Evans et al., 2004).

Variants in human *FGF12* have been linked to cognitive decline (Mohammadnejad et al., 2020), major depression (GENDEP Investigators et al., 2013), schizophrenia (Stertz et al., 2021), and sleep quality (Byrne et al., 2013). Recent evidence also supports the druggability of other intracellular FGFs, such as FGF14 (Dvorak et al., 2025; Singh et al., 2025) and FGF13 (Singh et al., 2025), through their interactions with sodium channels. Our findings suggest that FGF12 could represent a novel therapeutic target for OUD by modulating its interaction with sodium channels.

The epistasis of morphine locomotor activation

We identified a highly significant epistatic interaction between the *Oprm1* and *Fgf12* loci 45–90 min after morphine injection (Figure 6), that erodes in the following 30 mins, providing strong pharmacological constraints on mechanisms. Those strains that inherit both the *B/B* genotype at *Oprm1* and the *D*/D genotype at *Fgf12* have significantly higher activity levels compared to those strains that inherit the other three genotype combinations. Our mapping extends in intervals of 15 minutes over a 3 hour period. We can divide this interval into four phases (Figure 1).The first phase after the morphine injection is influenced only by DNA variants in the *Oprm1* locus. The second phase— from 45 to 90 minutes—is characterized by the strong but transient epistatic interaction of *Oprm1* and *Fgf12* loci. The third phase is a kind of hiatus that extends from 90 to 120 minutes in which we do not detect any epistatic interactions. Only *Oprm1* is active during this phase. In the final phase—from 120 to 180 minutes—the *Oprm1* effect is exhausted and now the *Fgf12* locus acts independently for the first time with a purely additive effect on activity. The hiatus phase may be explained mechanistically by effects of other loci that we are not yet able to detect reliably. Note for example the transient female-specific locus on Chr 5 that fills part of the hiatus. This complex time course of transitioning in genetic control on morphine induced locomotion is likely caused by molecular cascades triggered by the activation of the *OPRM1* receptor and its signalling molecules and downstream molecular network linked to *FGF12*. To some extent we have tried to bridge the gap between the genetics of morphine responses to possible molecular cascades using Bayesian causal modeling as in Figure 8.

Complex traits, such as OUD, are controlled by many genes that interact with each other and their environment (Crist et al., 2019). While improved statistical approaches (D'Silva et al., 2022; Wei et al., 2014) and novel machine learning methods (Chicco and Faultless, 2021) are starting to enable the study of epistasis in human data, most human genetic studies either did not have the power to detect epistasis or ignored its effect (Carlborg and Haley, 2004; Uffelmann et al., 2021). In contrast, many epistatic interactions have been identified using model organisms (Mackay, 2014), mostly due to the ability to obtain data from individuals with controlled genotypes and measuring phenotypes in well controlled environments (Campbell et al., 2018). Identifying gene-gene interactions in model organisms can provide candidates to be evaluated in the human population for its potential in improving the prediction of individual disease risk and the application of personalized therapies.

Cell-type specific gene expression in NAc

While gene interaction is nearly always measured statistically without regard to biological mechanism, we explored the utility of snRNA-seq in identifying cellular and molecular mechanisms of this interaction by examining gene expression in NAc, a brain region relevant to the biological effect of morphine. We focused on NAc because differences in morphine-induced dopamine release in NAc correspond with the locomotor response in the parental strains of the BXD mice (Murphy et al., 2001). Further, mice lacking *Drd1* are not responsive to acute cocaine-(Karlsson et al., 2008; Xu et al., 1994) or morphine-(Wang et al., 2015) induced locomotor response. While our analysis identified 17 distinctive cell types (Figure 7a), *Oprm1* was detected almost exclusively in the D1-MSN-3 subtype that have high expression of *Foxp2* and low expression of *Ppp1r1b* (i.e. *Darpp-32*; Figure 7b,c). The total number of genes (n_feature RNA) and other quality control (QC) parameters in D1-MSN-3 are comparable with other neuronal cell types. In contrast, *Fgf12* was expressed in most of the neuronal and glial cell types (Figure 7d). The expression level of *Oprm1* and *Fgf12* were positively correlated (r = 0.36, p = 6e-8) in D1-MSN-3 but not in D1-MSN-2 cells, indicating a potential cell-type specific mechanism for the epistatic interaction.

MSNs in the NAc have been the subject of intense research. A recent snRNA-seq study of the NAc in rat brains also detected this specific subtype expressing high levels of *Oprm1*, which is selectively labeled by the expression of *Chst9* (Andraka et al., 2023; Savell et al., 2020). These data suggest that D1-MSN-3 is a highly likely location for the interaction between *Orpm1* and *Fgf12*. Notably, this cell type is conserved also in primate and human NAc snRNA-seq data (Andraka et al., 2023), suggesting that it may play a critical role in opioid responses across species.

To further confirm our results and allow for analysis of correlations, we queried data from the *Ratlas* (*https://day-lab.shinyapps.io/ratlas/*), which reveals that *Fgf12* is indeed widely expressed in all cell types in other datasets, and that *Oprm1* was not detected in either *Drd1* or *Drd2* MSN neurons. This is most likely due to the lack of detection of the MSN subclass that is equivalent to the D1-MSN-3 subtype that we identified (Supplementary Figure 5a-d). However, cultured cell data do express *Oprm1* in both *Drd1* and *Drd2* cells (Supplementary Figure 5e-f). While out of the scope of this paper, future work will be needed to assess the impact of the *Oprm1-Fgf12* interaction on the activity of the D1-MSN-3 population in mediating opioid responses.

Bayesian causal network modeling of *OPRM1* and *FGF12*

We included gene expression data of several MAP kinases and sodium channels with known relationships with *Oprm1* and *Fgf12* as the input for our BN. The resulting network (Figure 8) indicated that *Mapk8ip2*, *Mapk3k11* (*Mlk3*), and *Map3k12* (*Dlk*) form a highly interactive network mediating the interaction between *Oprm1* and *Fgf12* in regulating their effects on morphine-induced locomotor response. In addition to validating the results on genetic influence on *Oprm1* and *Fgf12* expression and morphine-induced locomotor response, the network identified *Map3k11* as a potential nexus that links *Oprm1* and *Fgf12*. *Map3k11* further activates other MAP kinases such as *Mapk8ip2* and *Map3k12* to modulate locomotion before 120 min. Thus, *Map3k11* is a potential mediator of the epistasis between *Oprm1* and *Fgf12*. Our BN did not contain a direct relationship between *Fgf12* and *Mapk8ip2*, the encoded proteins for which directly bind to each other (Bhushan et al., 2017). It is possible that these two proteins do not regulate each other's mRNA levels, which was used in our BN. While our modeling suggest that the epistatic interaction between *Oprm1* and *Fgf12* is mediated through *Map3k11*, further research, such as those using Mendelian randomization studies and other forms of mediation analysis, could provide further understanding of the interactions between MAP kinases, *FGF12*, and *OPRM1*.

Genetic modulation of naloxone effects

Naloxone is a potent opioid antagonist that reverses opioid overdoses (Theriot et al., 2022), and is often used in treatment settings or as a primary overdose prevention method.

Pharmacogenomics has primarily focused on individualized treatment for pain, with less priority on OUD. However, understanding the role genetics plays in naloxone's mechanism could initiate potentially more personalized and effective treatments for OUD. We identified multiple significant associations between behavioral measures of the effect of naloxone on Chrs 3, 5, 7, 10, 11, 12, 13, 14, and 18. These loci are likely to contain novel genes that play a role in OUD. For example, *Slc7a7* and *Slc7a8* are candidate genes for the number of jumps after naloxone injection. Both of these genes are a part of the solute carrier family, which play a large role in the absorption of drugs and xenobiotics (Lin et al., 2015), and are expressed in the brain.

Similar to the morphine locomotion time series phenotypes, there are significant QTL for the differences in locomotion before and after naloxone injection (Figure 8c-d) on Chrs 10 and 16. Mice with the *B* allele at the *Fgf12* locus still had elevated locomotion during 165-180 min compared to those with the *D* allele. Injection of naloxone eliminated the remaining effect of morphine and brought locomotion in both genotypes close to baseline level (Supplementary Figure 7). The difference in locomotion before vs after naloxone injection thus amplified the net effect of morphine at this late phase and further confirmed that this effect was mediated via the MOR. The highly significant association (–logP = 5.34 in males and –logP = 9.57 in females) between the Chr 16 locus and this phenotype provided a strong confirmation for its role in late phase response to morphine. Analysis of these genes in the homologous human regions in larger populations are needed to translationally confirm and extend the validity of these results.

Integration with human data

While our attempt to integrate murine data with human GWAS results demonstrated that the pipeline works, the lack of enrichment for the network in OUD GWAS could likely be due to the small sample size in the original human data for that specific SUD. This could also likely be due to the lack of data specification, such as the differences between examining physical dependence vs the development of OUD, initial use vs problematic use, and withdrawal vs relapse (Sanchez-Roige et al., 2021).

In summary, our study confirmed that the *Oprm1* locus strongly modulates the early phase locomotor response to morphine and identified a novel association between *Fgf12* locus and the late phase response to morphine. To the best of our knowledge, the epistatic interaction between the *Oprm1* and *Fgf12* loci during the middle phase of locomotor response is the first demonstration of a transient time-dependent epistatic interaction modulating drug response in mammals—a finding with interesting mechanistic implications. Our snRNA-seq analysis suggests that the D1-MSN-3 subpopulation of dopaminergic-receptor neurons might be critical in the epistatic interaction between *Oprm1* and *Fgf12*. Our study further shows that the interaction between the *Fgf12* and *Oprm1* genes is mediated by *Mapk8ip2*, *Map3k11*, and *Map3k12*, and that the activity of these proteins is modulated by the presence of *Fgf12* variants. Finally, this work demonstrates how high-quality Findabile, Accessible, Interoperabile, and Reusable (FAIR+) phenotypes can be used with updated data sets to yield striking results, and how joint mouse and human neurogenomic and GWAS results can be merged at gene and network levels for bidirectional validation of SUD variants and molecular networks.

Methods

Animal and Behavior Data Collection

Morphine-induced locomotor responses and naloxone-induced withdrawal were recorded for 64 BXD RI strains. All animals were young adults (8–9 weeks) reared at the Oak Ridge National Laboratory in 2007–2008. Detailed methods were reported in the original publication by Philip et al (2010). Briefly, the testing protocols included giving each mouse a single i.p. injection of morphine sulfate (50 mg/kg in isotonic saline at a volume of 10 ml/kg), followed by immediately placing the mice into an activity chamber (43.2 cm L × 43.2 cm W × 30.4 cm H, ENV-515, Med Associates, St Albans, VT, USA). Each chamber contained two sets of 16 photocells placed at 2.5 and 5 cm above the chamber floor. Activity was measured as photocell beam breaks and converted

into horizontal distance traveled (cm). This behavior and rearing were recorded for 3 h and were exported as the sum of 15 min bins. Then, each mice in these cases received an injection of naloxone (30 mg/kg in isotonic saline at a volume of 10 ml/kg, i.p.), and were immediately returned to the chambers for an additional 15 minutes. Naloxone's effects on locomotor activity levels, and signs of withdrawal were recorded for 15 minutes, including the number of jumps, fecal boli, urine puddles, wet dog shakes, instances of abdominal contraction, salivation, ptosis and abnormal posture were recorded for 15 minutes). The number of animals used per strain was 7.8 (mean ± SD) for females and 6.6 for males. Testing occurred at about 8 to 9 weeks after birth.

QTL Mapping in GeneNetwork

We reanalyzed 105 phenotypes from the Philip et al. (2010) study available in *Genenetwork.org*, a database containing phenotypes and genotypes, and also serves as an analysis engine for quantitative trait locus (QTL) mapping, genetic correlations, and phenome-wide association studies (Mulligan et al., 2017; Sloan et al., 2016; Watson and Ashbrook, 2020). The trait IDs and their most significant loci are shown in Supplementary Table 2. The data for mapping QTLs consist of polymorphic genetic markers and quantitative trait values for strain means. Statistical heritability was also evaluated to estimate the degree of variation among the morphine and naloxone traits due to genetic variation. The original analysis (Philip et al., 2010) was performed with the expanded BXD strain to evaluate complementary behavioral phenotyping using Haley-Knott regression in GeneNetwork. In our reanalysis, we first quantile normalized the trait data. We then used the newly implemented GEMMA (Zhou and Stephens, 2012) with the LOCO option, which corrects family structure, to perform genetic mapping using approximately 7,000 markers obtained from whole genome sequencing. Candidate genes were selected from the confidence interval of a one-LOD drop-off from the peak statistical significance as determined previously (Philip et al., 2010). The criterion for genome-wide significance was a –logP value of 3.77 for the BXDs. Loci labeled by genetic markers could act independently at all time points or possibly in an epistatic interaction at a few time points.

Therefore, we also examined epistatic interactions between two loci by performing a pair-scan, implemented in GeneNetwork (v1). This scan generated a matrix map output. Functional enrichment of these networks were obtained using WebGestalt (Zhang et al., 2005). The biological relevance of candidate genes in the context of SUD was queried using Genecup (Gunturkun et al., 2022). We conducted most early exploratory analysis using the web version of Genenetwork. For final analysis, we used the API interface of genenetwork (Mulligan et al., 2017) to conduct standardized analysis and generate uniform figures for all phenotypes of interest.

Brain samples for snRNA-seq

Brain samples from 2 female HS rats were obtained from the oxycodone tissue repository at UCSD (Carrette et al., 2021). These rats were selected based on their low addiction-linked behavior phenotypes from a larger cohort characterized in the oxycodone self-administration paradigm. The brain tissues were collected from rats euthanized after 4 weeks of prolonged abstinence from oxycodone intravenous self-administration (Carrette et al., 2021). Brain tissue was extracted and snap-frozen (at −30°C). Cryosections of ~500 µm (Bregma 2.28-0.72 mm) were used to dissect the NAc core punches on a −20°C frozen stage. Punches from 3 sections were combined for each rat.

snRNA-seq library preparations

snRNA-seq library was performed using the Chromium Next GEM Single Cell Multiome Reagent Kit A (catalog number 1000282) following Chromium Next GEM Single Cell Multiome ATAC + Gene Expression Reagent Kits User Guide (10X Genomics). Approximately 10,000 nuclei were loaded per reaction, targeting recovery of 6,000 nuclei after encapsulation. After the transposition reaction, nuclei were encapsulated and barcoded. Next-generation sequencing libraries were constructed following the User Guide. Final library concentration was assessed by Qubit dsDNA HS Assay Kit

(Thermo-Fischer Scientific) and post library QC was performed using Tapestation High Sensitivity D1000 (Agilent) to ensure that fragment sizes were distributed as expected. Final libraries were sequenced using the NovaSeq6000 (Illumina).

Bioinformatic analysis of snRNA-seq data

Raw sequencing data were converted to FASTQ format using bcl2fastq (Illumina). The FASTQ data were firstly aligned to the Rattus Norvegicus mRatBN7.2/rn7 genome and then aggregated into one sample file using CellRanger version 2.0.0 using default parameters. The output files were analyzed using Seurat version 4.1.1 (Stuart et al., 2019). Nuclei with gene numbers between 500 and 6000, RNA counts between 1000 and 16000, the percentage of mitochondrial gene reads lower than 2%, and the percentage of small 40S or large 60S ribosomal (Rps and Rpl) gene reads lower than 1% were considered as high-quality cells and kept for further analyses. To eliminate potential doublets, we used DoubletFinder 2.0.3 and removed 5% nuclei identified as doublets (McGinnis et al., 2019).

High-quality singlet nuclei were then normalized and scaled using SCT transformation (Hafemeister and Satija, 2019) with the percentage of mitochondrial genes, RNA counts, and sample ID as covariates. The dimensional reduction was performed using PCA and the first 30 PCs were used for KNN graph construction and clustering using the Louvain algorithm. Uniform manifold approximation and projection (UMAP) was used for visualization of the clusters.

The dot plots and violin plots were generated using Seurat (Stuart et al., 2019). Pearson correlation was computed in R 4.2.1 using cor.test and $p<0.05$ was considered significant.

Human translational data

We reviewed OUD and other relevant published GWAS data in previous literature with variants in *OPRM1* and *FGF12*. We also extended our review to looking at potential roles of *FGF12* in humans specifically. Then, All the files for *FGF12* and *OPRM1* correlations for each individual brain region as well as some controls were downloaded using GTEx v8 (GTEx Consortium et al., 2017) and GeneNetwork and then extracted out the shared genes with a liberal cut-off of 500 genes. We ran a genome-wide enrichment analysis using MAGMA, a powerful tool that identifies genes and gene-sets associated with a specific disease for analysis (de Leeuw et al., 2015). However, upon running our genome-wide enrichment analysis for OUD, we realized our initial search was too broad and much larger than in previous literature (see results section). To reduce the amount of noise we identified genes that overlap between *FGF12* and *OPRM1* in a given tissue, and identified genes correlated specifically to each *OPRM1* and *FGF12* in several tissues. To do this we developed a list of genes (and Ensembl IDs) in each brain region to examine the number of occurrences each gene is seen across this data. We narrowed down our search to the top genes with high counts and compared them to the same number of genes with a count of only one. The count is the number of times the gene is associated with both *FGF12* and *OPRM1* in all the regions/tissue datasets in GeneNetwork. Association is defined as among the top 500 genes ranked by correlation with *FGF12* or *OPRM1*.

Bayesian network modeling

The BN server located at *https://bnw.genenetwork.org/sourcecodes/home.php* was used. Raw data files containing genotypes for the *Oprm1* and *Fgf12* loci, morphine-induced locomotion, and expression levels of relevant genes (sodium channels, MAP kinases) were transferred from Genentwork. We separated our nodes into 4 tiers to label chromosome location, candidate gene, signaling molecules, and phenotype (morphine locomotion) each as a separate tier.

These are used to organize the nodes into different layers. Each tier represents a different layer of complexity. We permitted causal connections to flow from the first tier to the second tier, as well as from the second tier to the third tier. We also allowed interaction between nodes located within the second or the third tiers.

Data availability

All behavioral data are available from *www.genenetwork.org* (see Table S2 for trait IDs). All snRNA-seq data have been deposited into NCBI GEO (accession number: GSE214388).

Supplementary Figures and Tables

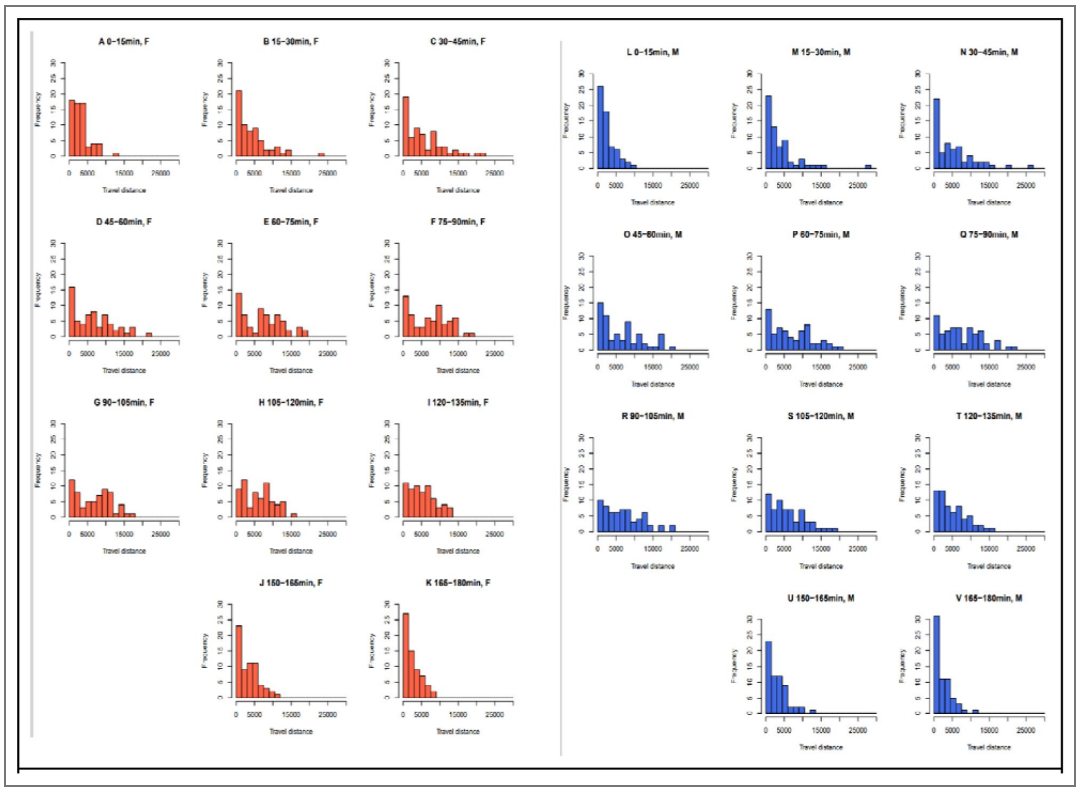

Supplementary Figure 1. Distribution of raw locomotion data after morphine injection. Distribution of raw data for locomotion after morphine injection at different time intervals in females (orange A-K) and males (blue L-V). Data for 135 to 150 minutes were lost for both sexes.

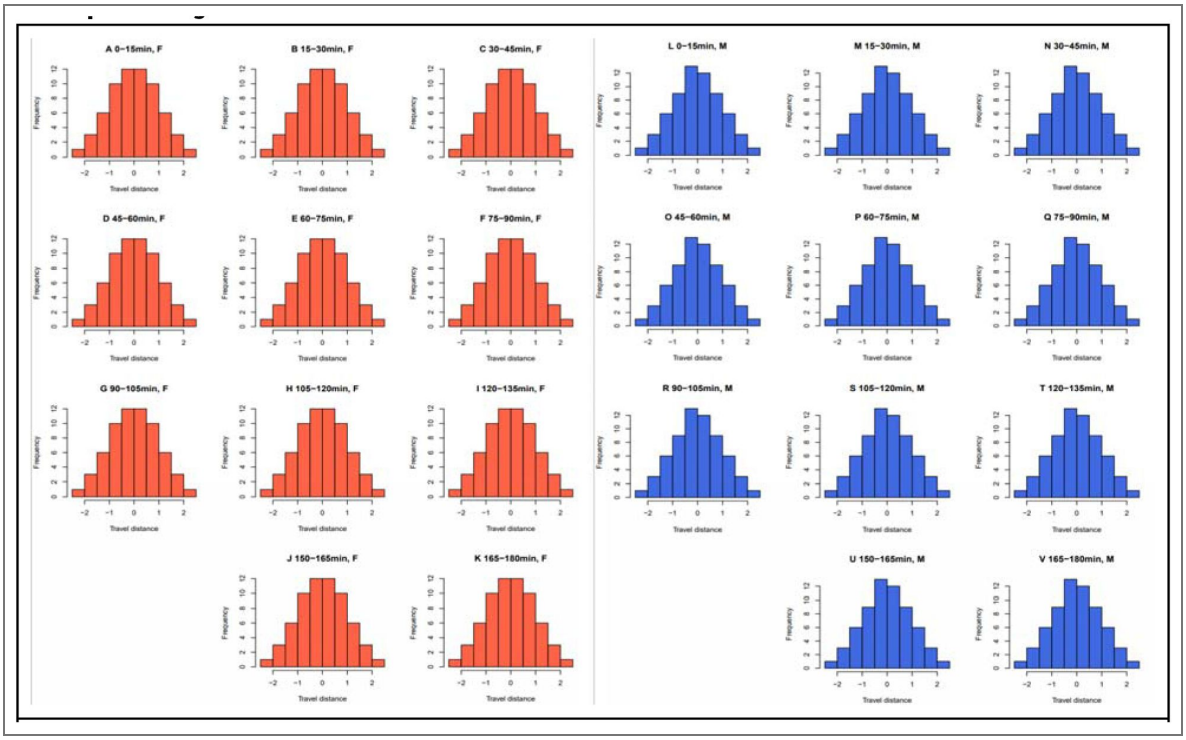

Supplementary Figure 2. Distribution of quantile-normalized locomotion data after morphine injection.

Data are plotted for each time bin for both females (orange A-K) and males (blue L-V). Data for 135 to 150 minutes were lost for both sexes.

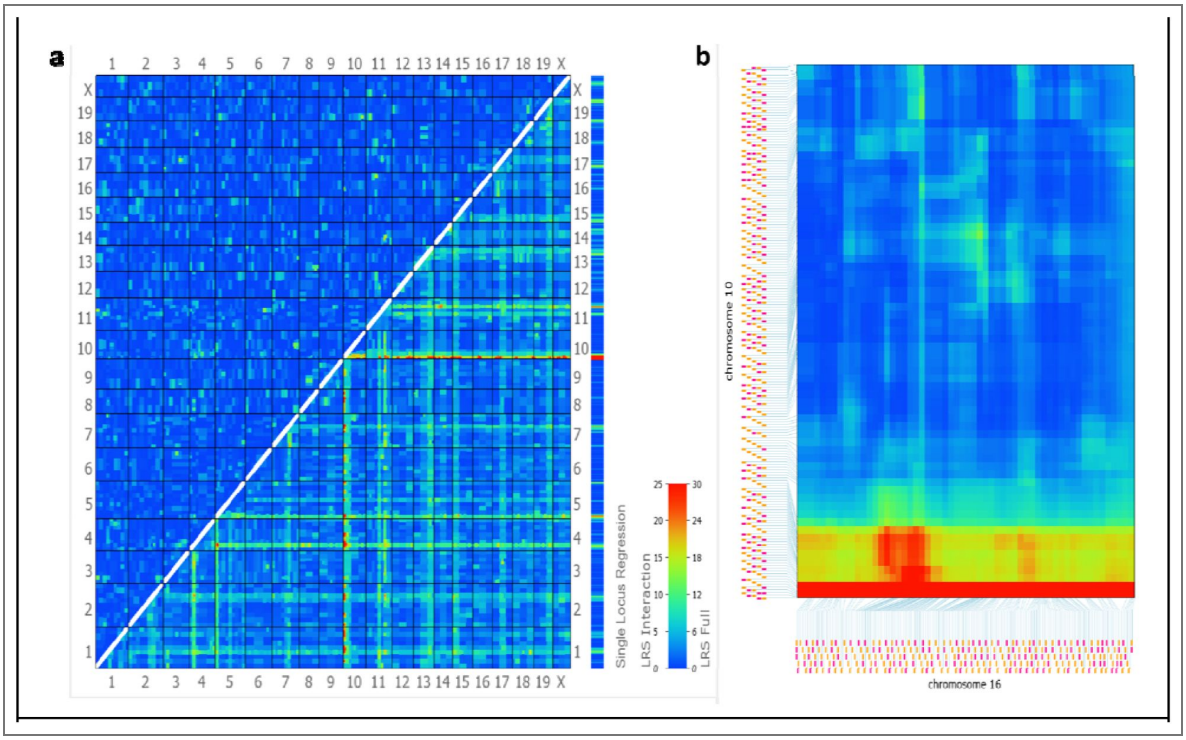

Supplementary Figure 3. Pairwise linkage statistics across the genome.

(a) Genome-wide two-dimensional heat map showing all pairwise marker combinations, illustrating both additive (main) effects and epistatic (interaction) effects. The upper-left triangle displays LOD scores for interaction terms, while the rightmost column shows the main effect (single-locus) genome scan. (b) Zoomed view of linkage statistics between chromosomes 10 and 16. The red band along the bottom represents a strong additive effect on chromosome 16.

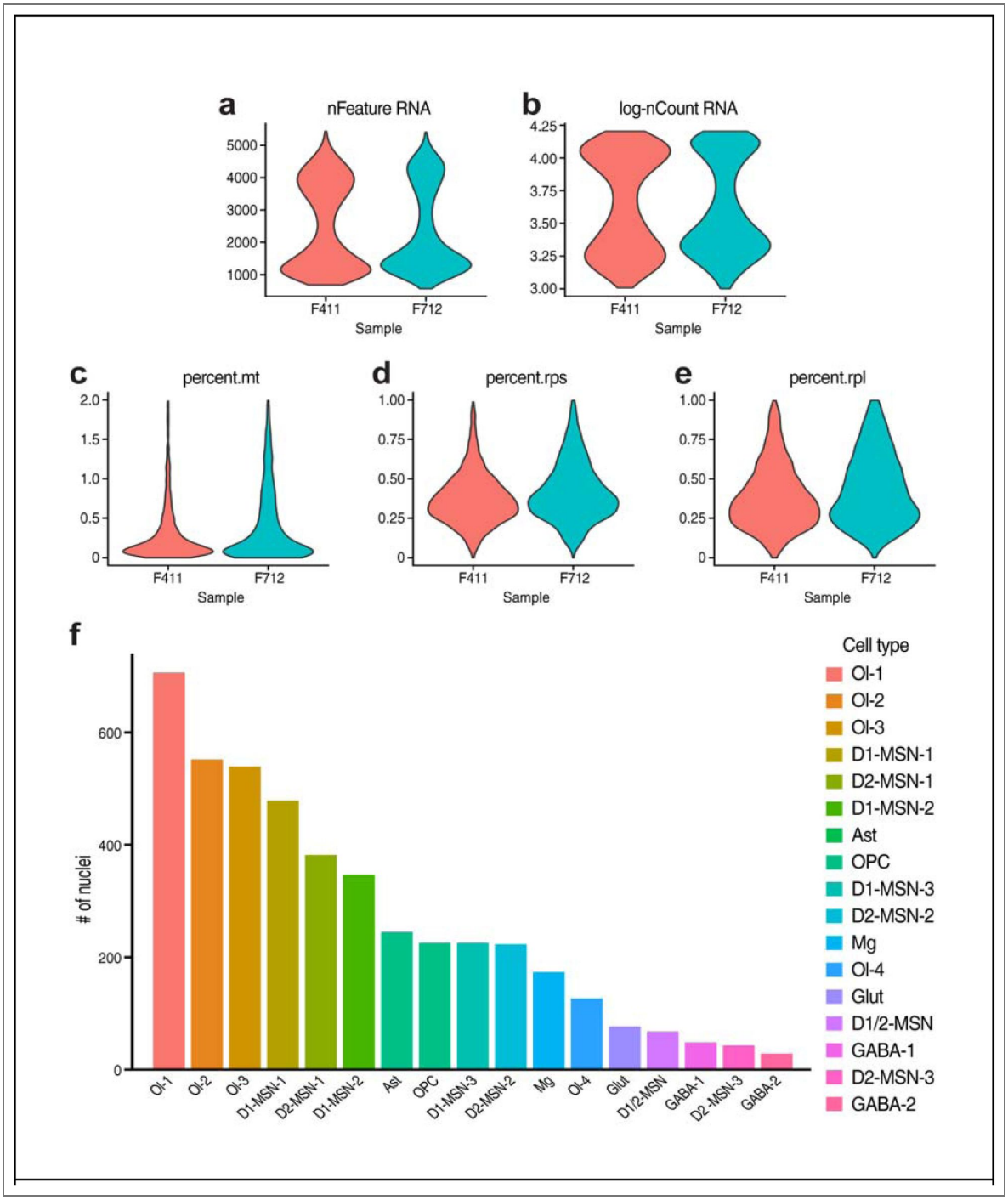

Supplementary Figure 4. Quality control (QC) of snRNA-seq and number of cells per cluster.

(a-e) Violin plots showing QC parameters used for selecting high-quality nuclei in each sample: (a) Unique gene numbers per nuclei (nFeature_RNA). (b) Log-transformed total read numbers per nuclei (log-nCount_RNA). (c) Percentage of mitochondrial gene reads. (d) Percentage of small 40s ribosomal (Rps) gene reads. (e) Percentage of large 60s ribosomal (Rpl) gene reads. (f) Number of nuclei per cell cluster. D1-MSN, Drd1-expressing medium spiny neuron; D2-MSN, Drd2-expressing medium spiny neuron; GABA, GABAergic inhibitory neuron; Glut, glutamatergic excitatory neuron; Ol, oligodendrocyte; OPC, oligodendrocyte precursor cell; Ast, astrocyte, Mg, microglial cells.

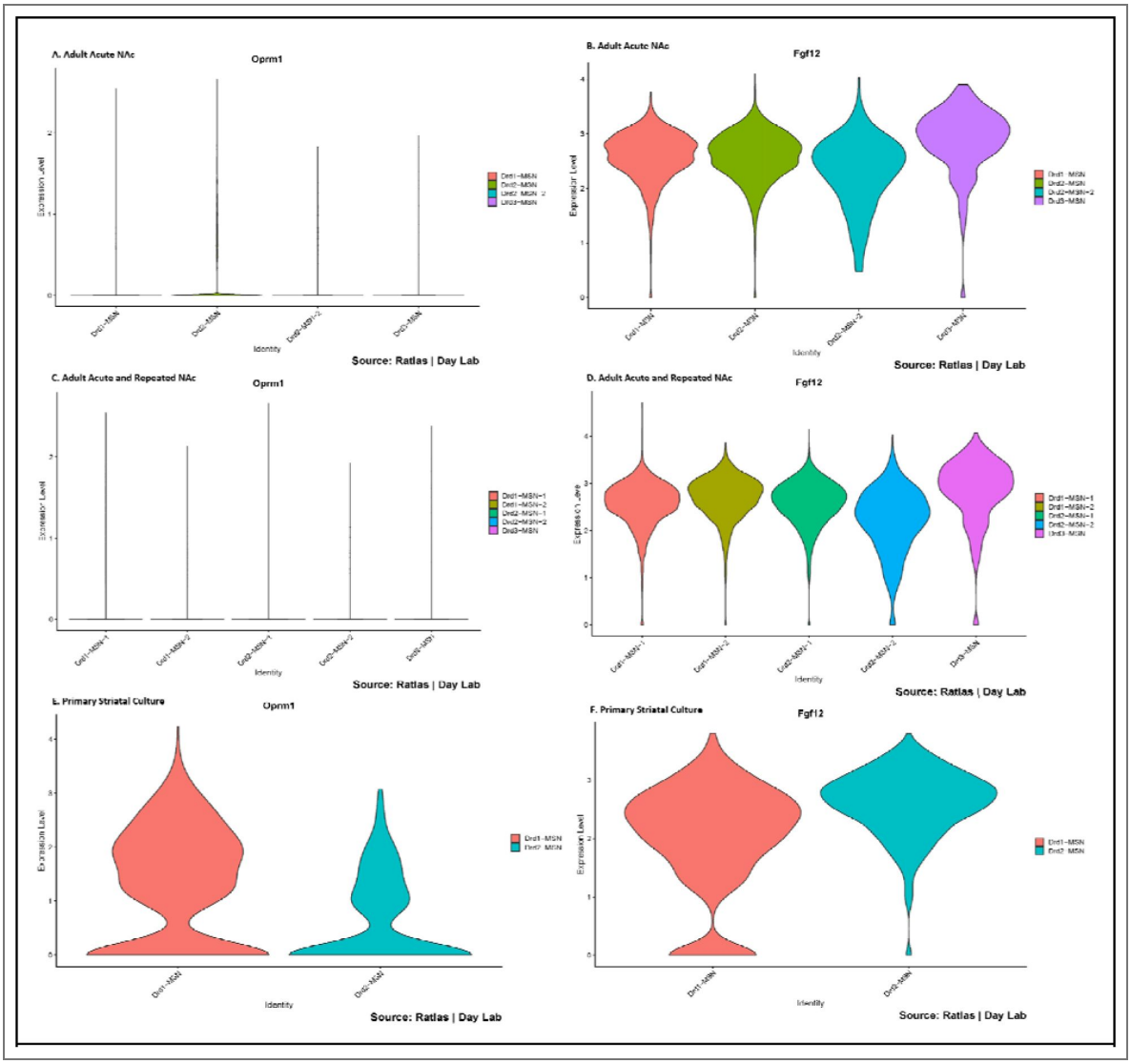

Supplementary Figure 5. Gene Expression of D1 and D2 Type Medium Spiny Neuron Subtypes.

Expression of Oprm1 and Fgf12 in acute and repeated nucleus accumbens and in primary striatal culture from the Ratlas database. (a) Expression of Oprm1 in acute NAc. (b) Expression of Fgf12 in acute NAc. (c) Expression of Oprm1 in both acute and repeated NAc. (d) Expression of Fgf12 in both acute and repeated NAc. (e) Expression of Oprm1 in primary striatal culture. (f) Expression of Fgf12 in primary striatal culture.

Supplementary Figure 6. Levels of Oprm1, Fgf12, and MAP kinases proteins in the brains of BXD parental strains and F1s.

Effect of genotype on associated MAP kinases and genes for both parental strains and F1 generations. The genotype effect shows the B allele is associated with high expression of Oprm1 and the MAP kinases Mapk8ip2, Map3k11, and Map3k12, but low expression of Fgf12, when compared to the D allele.

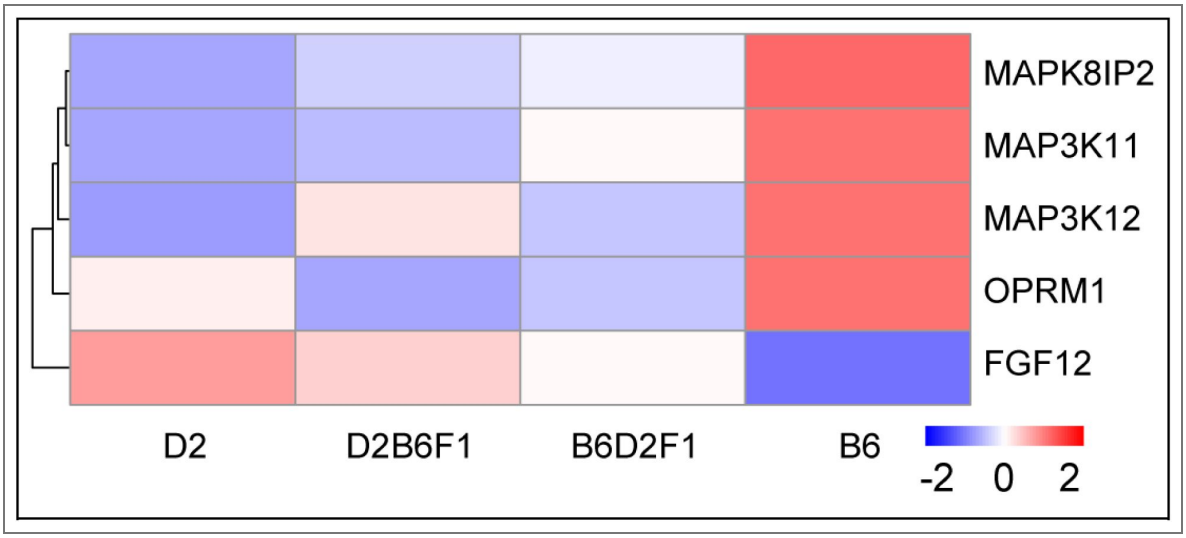

Supplementary Figure 7. Naloxone Phenotypes vs. Genotypes

The turquoise points show morphine-induced locomotion (distance traveled in cm) between 165–180 min after injection. Orange points show the change in locomotion measured by the last 15 min of morphine locomotion response minus the first 15 min after naloxone injection. (a) Effect of genotype on two naloxone phenotypes in males. (b) Effect of genotype on number of beam breaks in an open field 0–15 min after naloxone injection in males. (c) Effect of genotype on two naloxone phenotypes in females. (d) Effect of genotype on the number of beam breaks in an open field 0–15 min after naloxone injection in females.

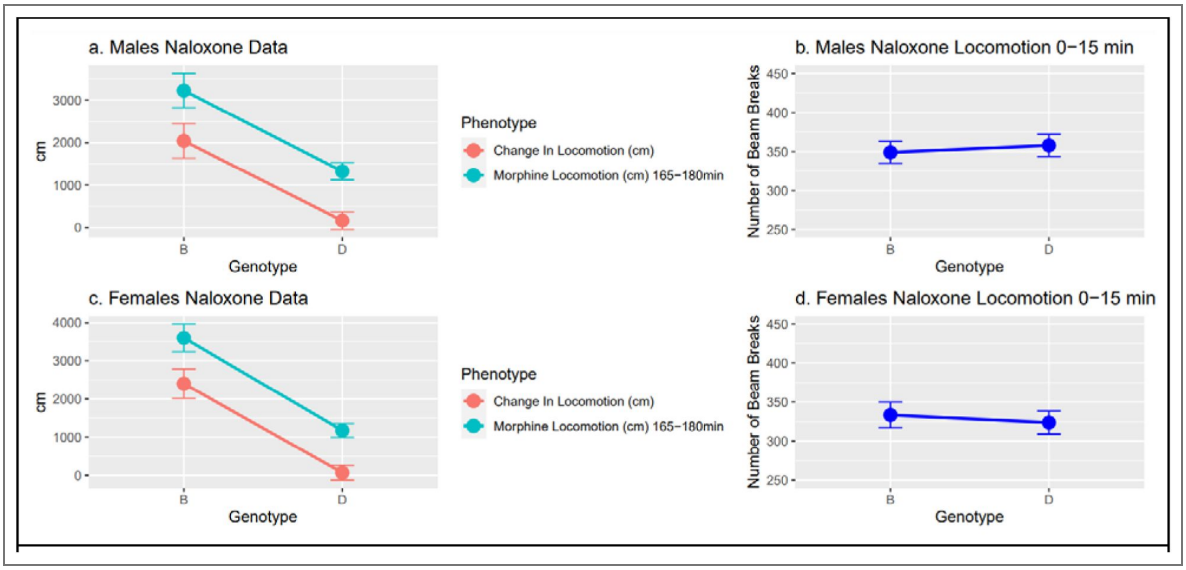

Locus	Peak LOD	Chr	Peak	Add Effect	Short description	Time	Sex ‡	N Strains	GN BXD Trait
Mor1a	3.99	1	74.07	-0.40	Morphine-induced locomotion, distance traveled	0-15	F	64	11583
Mor1a	3.95	1	74.07	-0.37	Morphine-induced locomotion, distance traveled	15-30	F	64	11586
Mor1a	4.42	1	77.64	-0.42	Morphine-induced locomotion, distance traveled	0-15	F	64	11583
Nalx1a	3.96	1	128.54	-0.43	Naloxone-induced withdrawal, salivation	NA	MF	64	11875
Nalx1b	4.14	1	167.17	-0.44	Naloxone-induced withdrawal, salivation	NA	MF	64	11875
Mor1b	4.32	1	173.53	-0.38	Morphine-induced locomotion, distance traveled	150-165	F	64	11584
Mor4a	4.06	4	21.69	-0.39	Morphine-induced locomotion, distance traveled	45-60	M	63	11331
Mor5a	3.84	5	9.85	0.41	Morphine-induced locomotion, distance traveled	60-75	F	64	11589
Mor5a	4.62	5	9.85	0.47	Morphine-induced locomotion, distance traveled	75-90	F	64	11590
Mor5a	4.49	5	9.85	0.48	Morphine-induced locomotion, distance traveled	90-105	F	64	11580
Mor5a	5.01	5	9.85	0.52	Morphine-induced locomotion, distance traveled	105-120	F	64	11581
Mor5a	4.11	5	9.85	0.47	Morphine-induced locomotion, distance traveled	120-135	F	64	11582
Mor5a	4.00	5	13.91	0.41	Morphine-induced locomotion, distance traveled	60-75	F	64	11589
Mor5a	3.80	5	13.91	0.40	Morphine-induced locomotion, distance traveled	45-60	F	64	11588
Mor5b	3.86	5	82.22	0.41	Morphine-induced locomotion, distance traveled	30-45	F	64	11587
Nalx6a	4.69	6	116.94	-0.42	Naloxone-induced withdrawal, horizontal activity	0-15	MF	64	11871
Nalx6a	4.65	6	116.94	-0.42	Naloxone-induced withdrawal, locomotion	0-15	MF	64	11870
Nalx6a	3.98	6	116.94	-0.39	Naloxone-induced withdrawal, horizontal activity	0-15	F	64	11614
Nalx6a	4.39	6	116.94	-0.41	Naloxone-induced withdrawal, locomotion	0-15	F	64	11613
Mor7a	3.88	7	84.15	-0.46	Morphine-induced locomotion, distance traveled	90-105	M	63	11323
Mor7a	5.28	7	96.83	-0.44	Morphine-induced locomotion, distance traveled	0-15	M	63	11326
Mor7a	3.89	7	96.83	-0.39	Morphine-induced locomotion, distance traveled	30-45	M	63	11330

Supplementary Table 1. Genome-wide significant loci associated with morphine and naloxone responses (quantile-normalized).

Mor7a	3.88	7	96.83	-0.39	Morphine-induced locomotion, distance traveled	45-60	M	63	11331
Mor7a	4.15	7	104.15	-0.48	Morphine-induced locomotion, distance traveled	45-60	M	63	11331
Mor7a	3.96	7	107.29	-0.43	Morphine-induced locomotion, distance traveled	45-60	M	63	11331
Mor7a	3.95	7	114.58	-0.34	Morphine-induced locomotion, distance traveled	30-45	F	64	11587
Mor9a	3.90	9	83.86	0.45	Morphine-induced locomotion, distance traveled	120-135	F	64	11582
Mor10a	9.46	10	4.94	-0.58	Morphine-induced locomotion, distance traveled	60-75	M	63	11332
Mor10a	8.12	10	4.94	-0.60	Morphine-induced locomotion, distance traveled	75-90	M	63	11333
Mor10a	4.02	10	4.94	-0.45	Morphine-induced locomotion, distance traveled	120-135	M	63	11325
Mor10a/ Nalx10a	4.33	10	5.61	-0.42	Naloxone-induced withdrawal, change in locomotion	NA	M	63	11339
Mor10a	10.53	10	5.64	-0.59	Morphine-induced locomotion, distance traveled	30-45	M	63	11330
Mor10a	10.06	10	5.64	-0.59	Morphine-induced locomotion, distance traveled	45-60	M	63	11331
Mor10a	4.23	10	8.90	-0.40	Morphine-induced locomotion, distance traveled	0-15	F	64	11583
Mor10a	3.80	10	8.90	-0.42	Morphine-induced locomotion, distance traveled	120-135	F	64	11582
Mor10a	4.07	10	8.90	-0.41	Morphine-induced locomotion, distance traveled	0-15	M	63	11326
Mor10a	5.05	10	8.90	-0.51	Morphine-induced locomotion, distance traveled	120-135	M	63	11325
Mor10a	4.60	10	8.90	-0.46	Morphine-induced locomotion, distance traveled	105-120	F	64	11581
Mor10a	6.86	10	8.90	-0.59	Morphine-induced locomotion, distance traveled	105-120	M	63	11324
Mor10a	8.52	10	8.90	-0.54	Morphine-induced locomotion, distance traveled	30-45	F	64	11587
Mor10a	6.44	10	8.90	-0.52	Morphine-induced locomotion, distance traveled	90-105	F	64	11580
Mor10a	9.30	10	8.90	-0.56	Morphine-induced locomotion, distance traveled	15-30	M	63	11329
Mor10a	7.79	10	8.90	-0.52	Morphine-induced locomotion, distance traveled	15-30	F	64	11586
Mor10a	9.60	10	8.90	-0.59	Morphine-induced locomotion, distance traveled	45-60	F	64	11588
Mor10a	9.58	10	8.90	-0.59	Morphine-induced locomotion, distance traveled	60-75	F	64	11589
Mor10a	8.34	10	8.90	-0.58	Morphine-induced locomotion, distance traveled	75-90	F	64	11590
Mor10a	7.51	10	8.90	-0.61	Morphine-induced locomotion, distance traveled	90-105	M	63	11323

Supplementary Table 1. (continued)

Mor10a	3.93	10	12.85	-0.43	Morphine-induced locomotion, distance traveled	90-105	F	64	11580
Nalx12a	3.83	12	27.59	0.39	Naloxone-induced withdrawal, locomotion	0-15	F	64	11613
Nalx12a	4.38	12	27.59	0.44	Naloxone-induced withdrawal, locomotion	0-15	MF	64	11870
Nalx12a	4.91	12	27.59	0.46	Naloxone-induced withdrawal, horizontal activity	0-15	MF	64	11871
Nalx12a	4.26	12	36.01	0.47	Naloxone-induced withdrawal, horizontal activity	0-15	F	64	11614
Mor12a	4.03	12	70.75	-0.42	Morphine-induced locomotion, distance traveled	0-15	F	64	11583
Mor12b	5.15	12	99.58	-0.45	Morphine-induced locomotion, distance traveled	0-15	F	64	11583
Mor12b	5.44	12	99.58	-0.43	Morphine-induced locomotion, distance traveled	15-30	F	64	11586
Mor12b	5.71	12	99.58	-0.44	Morphine-induced locomotion, distance traveled	30-45	F	64	11587
Mor12b	5.60	12	99.58	-0.43	Morphine-induced locomotion, distance traveled	65-70	F	64	11589
Mor12b	3.94	12	99.58	-0.39	Morphine-induced locomotion, distance traveled	75-90	F	64	11590
Mor12b	4.01	12	104.28	-0.40	Morphine-induced locomotion, distance traveled	15-30	F	64	11586
Nalx14a	4.00	14	52.13	-0.41	Naloxone-induced withdrawal, number of jumps	NA	M	63	11336
Nalx14b	4.25	14	118.46	-0.24	Naloxone-induced withdrawal locomotion	0-15	MF	64	11870
Nalx14b	4.36	14	118.46	-0.25	Naloxone-induced withdrawal, horizontal activity	0-15	MF	64	11871
Mor16a/ Nalx16a	5.34	16	27.45	-0.47	Naloxone-induced withdrawal, change in locomotion	NA	M	63	11339
Mor16a/ Nalx16a	10.56	16	27.45	-0.61	Morphine-induced locomotion, distance traveled	165-180	F	64	11585
Mor16a/ Nalx16a	4.28	16	27.45	-0.45	Morphine-induced locomotion, distance traveled	165-180	M	63	11328
Mor16a/ Nalx16a	5.83	16	28.99	-0.51	Morphine-induced locomotion, distance traveled	150-165	F	64	11584
Mor16a/ Nalx16a	3.92	16	28.99	-0.44	Morphine-induced locomotion, distance traveled	165-180	M	63	11328
Nalx16b	4.02	16	59.72	0.42	Naloxone-induced withdrawal, salivation	NA	MF	64	11875

‡ MF = male and female joint mapping. M / F = significant in both sexes but –logP value applies to first entry

Supplementary Table 1. (continued)

Sex	Time (min)	TraitID

Supplementary Table 2. **List of Locomotion Trait IDs.**

females	0-15	BXD_11583
females	15-30	BXD_11586
females	30-45	BXD_11587
females	45-60	BXD_11588
females	60-75	BXD_11589
females	75-90	BXD_11590
females	90-105	BXD_11580
females	105-120	BXD_11581
females	120-135	BXD_11582
females	150-165	BXD_11584
females	165-180	BXD_11585
males	0-15	BXD_11326
males	15-30	BXD_11329
males	30-45	BXD_11330
males	45-60	BXD_11331
males	60-75	BXD_11332
males	75-90	BXD_11333
males	90-105	BXD_11323
males	105-120	BXD_11324

Supplementary Table 2. (continued)

males	120-135	BXD_11325
males	150-165	BXD_11327
males	165-180	BXD_11328

Supplementary Table 2. (continued)

Additional information

Funding

Funder	Grant reference number	Author
National Institute of Development Administration (NIDA)	U01DA053672	Robert Williams Hao Chen

Author ORCID iDs

Paige M Lemen: https://orcid.org/0000-0002-1774-0385
Alexander S Hatoum: https://orcid.org/0000-0002-8002-7267
Price E Dickson: https://orcid.org/0000-0003-3153-0170
Arpana Agrawal: https://orcid.org/0000-0002-0313-793X
Benjamin C Reiner: https://orcid.org/0000-0001-7796-587X
Wade Berrettini: https://orcid.org/0000-0002-4733-2286
David G Ashbrook: https://orcid.org/0000-0002-7397-8910
Mustafa Hakan Gunturkun: https://orcid.org/0000-0003-0612-6432
Megan K Mulligan: https://orcid.org/0000-0003-4909-635X
Caleb J Browne: https://orcid.org/0000-0003-0089-5433
Eric J Nestler: https://orcid.org/0000-0002-7905-2000
Robert W Williams: https://orcid.org/0000-0001-8924-4447
Hao Chen: https://orcid.org/0000-0002-2680-6921

References

Andraka E, Phillips RA, Brida KL, Day JJ. (2023) Chst9 Marks a Spatially and Transcriptionally Unique Population of Oprm1-Expressing Neurons in the Nucleus Accumbens. *bioRxiv* https://doi.org/10.1101/2023.10.16.562623 | PubMed

Ashbrook DG, Arends D, Prins P, Mulligan MK, Roy S, Williams EG, Lutz CM, Valenzuela A, Bohl CJ, Ingels JF, *et al.* (2021) A platform for experimental precision medicine: The extended BXD mouse family. *Cell Syst* **12**:235-247. https://doi.org/10.1016/j.cels.2020.12.002 | PubMed

Ballester J, Baker AK, Martikainen IK, Koppelmans V, Zubieta J-K, Love TM (2022) Risk for opioid misuse in chronic pain patients is associated with endogenous opioid system dysregulation. *Transl Psychiatry* **12**:20 https://doi.org/10.1038/s41398-021-01775-z | PubMed

Bergeson SE, Helms ML, O'Toole LA, Jarvis MW, Hain HS, Mogil JS, Belknap JK (2001) Quantitative trait loci influencing morphine antinociception in four mapping populations. *Mamm Genome* **12**:546-553 https://doi.org/10.1007/s003350020022 | PubMed

Berrettini W (2017) A brief review of the genetics and pharmacogenetics of opioid use disorders. *Dialogues Clin Neurosci* **19**:229-236 https://doi.org/10.31887/dcns.2017.19.3/wberrettini | PubMed

Bhushan A, Singh A, Kapur S, Borthakar BB, Sharma J, Rai AK, Kataki AC, Saxena S (2017) Identification and Validation of Fibroblast Growth Factor 12 Gene as a Novel Potential Biomarker in Esophageal Cancer Using Cancer Genomic Datasets. *Omics* **21**:616-631 https://doi.org/10.1089/omi.2017.0116 | PubMed

Blackwood CA, Leary M, Salisbury A, McCoy MT, Cadet JL (2019) Escalated Oxycodone Self-Administration Causes Differential Striatal mRNA Expression of FGFs and IEGs Following Abstinence-Associated Incubation of Oxycodone Craving. *Neuroscience* **415**:173-183 https://doi.org/10.1016/j.neuroscience.2019.07.030 | PubMed

Buchsbaum RJ, Connolly BA, Feig LA (2002) Interaction of Rac exchange factors Tiam1 and Ras-GRF1 with a scaffold for the p38 mitogen-activated protein kinase cascade. *Mol Cell Biol* **22**:4073-4085 https://doi.org/10.1128/mcb.22.12.4073-4085.2002 | PubMed

Byrne EM, Gehrman PR, Medland SE, Nyholt DR, Heath AC, Madden PAF, Hickie IB, Van Duijn CM, Henders AK, Montgomery GW, *et al.* (2013) A genome-wide association study of sleep habits and insomnia. *Am J Med Genet B Neuropsychiatr Genet* 162B https://doi.org/10.1002/ajmg.b.32168 | PubMed

Campbell RF, McGrath PT, Paaby AB (2018) Analysis of Epistasis in Natural Traits Using Model Organisms. *Trends Genet* **34**:883-898 https://doi.org/10.1016/j.tig.2018.08.002 | PubMed

Carlborg O, Haley CS (2004) Epistasis: too often neglected in complex trait studies?. *Nat Rev Genet* **5**:618-625 https://doi.org/10.1038/nrg1407 | PubMed

Carrette LLG, de Guglielmo G, Kallupi M, Maturin L, Brennan M, Boomhower B, Conlisk D, Sedighim S, Tieu L, Fannon MJ, *et al.* (2021) The Cocaine and Oxycodone Biobanks, Two Repositories from Genetically Diverse and Behaviorally Characterized Rats for the Study of Addiction. *eNeuro* **8** https://doi.org/10.1523/ENEURO.0033-21.2021 | PubMed

Cheng Z, Zhou H, Sherva R, Farrer LA, Kranzler HR, Gelernter J (2018) Genome-wide Association Study Identifies a Regulatory Variant of RGMA Associated With Opioid Dependence in European Americans. *Biol Psychiatry* https://doi.org/10.1016/j.biopsych.2017.12.016 | PubMed

Chicco D, Faultless T (2021) Brief Survey on Machine Learning in Epistasis. *Methods Mol Biol* **2212**:169-179 https://doi.org/10.1007/978-1-0716-0947-7_11 | PubMed

Contet C, Kieffer BL, Befort K (2004) Mu opioid receptor: a gateway to drug addiction. *Curr Opin Neurobiol* **14**:370-378 https://doi.org/10.1016/j.conb.2004.05.005 | PubMed

Cox JW, Sherva RM, Lunetta KL, Johnson EC, Martin NG, Degenhardt L, Agrawal A, Nelson EC, Kranzler HR, Gelernter J, *et al.* (2020) Genome-Wide Association Study of Opioid Cessation. *J Clin Med Res* **9** https://doi.org/10.3390/jcm9010180 | PubMed

Crist RC, Reiner BC, Berrettini WH (2019) A review of opioid addiction genetics. *Curr Opin Psychol* **27**:31-35 https://doi.org/10.1016/j.copsyc.2018.07.014 | PubMed

Crocco P, Dato S, La Grotta R, Passarino G, Rose G. (2024) Evidence for a relationship between genetic polymorphisms of the L-DOPA transporter LAT2/4F2hc and risk of hypertension in the context of chronic kidney disease. *BMC Med Genomics* **17**:163 https://doi.org/10.1186/s12920-024-01935-2 | PubMed

Cui Y, Ostlund SB, James AS, Park CS, Ge W, Roberts KW, Mittal N, Murphy NP, Cepeda C, Kieffer BL, *et al.* (2014) Targeted expression of μ-opioid receptors in a subset of striatal direct-pathway neurons restores opiate reward. *Nat Neurosci* **17**:254-261 https://doi.org/10.1038/nn.3622 | PubMed

Deak JD, Zhou H, Galimberti M, Levey DF, Wendt FR, Sanchez-Roige S, Hatoum AS, Johnson EC, Nunez YZ, Demontis D, *et al.* (2022) Genome-wide association study in individuals of European and African ancestry and multi-trait analysis of opioid use disorder identifies 19 independent genome-wide significant risk loci. *Mol Psychiatry* **27**:3970-3979 https://doi.org/10.1038/s41380-022-01709-1 | PubMed

de Leeuw CA, Mooij JM, Heskes T, Posthuma D (2015) MAGMA: generalized gene-set analysis of GWAS data. *PLoS Comput Biol* **11**:e1004219 https://doi.org/10.1371/journal.pcbi.1004219 | PubMed

De Vries TJ, Shippenberg TS. (2002) Neural systems underlying opiate addiction. *J Neurosci* **22**:3321-3325 https://doi.org/10.1523/jneurosci.22-09-03321.2002 | PubMed

D'Silva S, Chakraborty S, Kahali B (2022) Concurrent outcomes from multiple approaches of epistasis analysis for human body mass index associated loci provide insights into obesity biology. *Sci Rep* **12**:7306 https://doi.org/10.1038/s41598-022-11270-0 | PubMed

Dvorak NM, Wadsworth PA, Aquino-Miranda G, Wang P, Engelke DS, Zhou J, Nguyen N, Singh AK, Aceto G, Haghighijoo Z, *et al.* (2025) Enhanced motivated behavior mediated by pharmacological targeting of the FGF14/Na1.6 complex in nucleus accumbens neurons. *Nat Commun* **16**:110 https://doi.org/10.1038/s41467-024-55554-7 | PubMed

Evans SJ, Choudary PV, Neal CR, Li JZ, Vawter MP, Tomita H, Lopez JF, Thompson RC, Meng F, Stead JD, *et al.* (2004) Dysregulation of the fibroblast growth factor system in major depression. *Proc Natl Acad Sci U S A* **101**:15506-15511 https://doi.org/10.1073/pnas.0406788101 | PubMed

Even-Chen O, Barak S (2019a) The role of fibroblast growth factor 2 in drug addiction. *Eur J Neurosci* **50**:2552-2561 https://doi.org/10.1111/ejn.14133 | PubMed

Even-Chen O, Barak S (2019b) Inhibition of FGF Receptor-1 Suppresses Alcohol Consumption: Role of PI3 Kinase Signaling in Dorsomedial Striatum. *J Neurosci* **39**:7947-7957 https://doi.org/10.1523/jneurosci.0805-19.2019 | PubMed

Even-Chen O, Sadot-Sogrin Y, Shaham O, Barak S (2017) Fibroblast Growth Factor 2 in the Dorsomedial Striatum Is a Novel Positive Regulator of Alcohol Consumption. *J Neurosci* **37**:8742-8754 https://doi.org/10.1523/jneurosci.0890-17.2017 | PubMed

Flippo KH, Trammell SAJ, Gillum MP, Aklan I, Perez MB, Yavuz Y, Smith NK, Jensen-Cody SO, Zhou B, Claflin KE, *et al.* (2022) FGF21 suppresses alcohol consumption through an amygdalo-striatal circuit. *Cell Metab* **34**:317-328. https://doi.org/10.1016/j.cmet.2021.12.024 | PubMed

Flores JA, Galan-Rodriguez B, Rojo AI, Ramiro-Fuentes S, Cuadrado A, Fernandez-Espejo E (2010) Fibroblast growth factor-1 within the ventral tegmental area participates in motor sensitizing effects of morphine. *Neuroscience* **165**:198-211 https://doi.org/10.1016/j.neuroscience.2009.10.009 | PubMed

Gaddis N, Mathur R, Marks J, Zhou L, Quach B, Waldrop A, Levran O, Agrawal A, Randesi M, Adelson M, *et al.* (2022) Multi-trait genome-wide association study of opioid addiction: OPRM1 and beyond. *Sci Rep* **12**:16873 https://doi.org/10.1038/s41598-022-21003-y | PubMed

Gelernter J, Kranzler HR, Sherva R, Koesterer R, Almasy L, Zhao H, Farrer LA (2014) Genome-wide association study of opioid dependence: multiple associations mapped to calcium and potassium pathways. *Biol Psychiatry* **76**:66-74 https://doi.org/10.1016/j.biopsych.2013.08.034 | PubMed

GENDEP Investigators, MARS Investigators, STAR*D Investigators (2013) Common genetic variation and antidepressant efficacy in major depressive disorder: a meta-analysis of three genome-wide pharmacogenetic studies. *Am J Psychiatry* **170**:207-217 https://doi.org/10.1176/appi.ajp.2012.12020237 | PubMed

Goldfarb M, Schoorlemmer J, Williams A, Diwakar S, Wang Q, Huang X, Giza J, Tchetchik D, Kelley K, Vega A, *et al.* (2007) Fibroblast growth factor homologous factors control neuronal excitability through modulation of voltage-gated sodium channels. *Neuron* **55**:449-463 https://doi.org/10.1016/j.neuron.2007.07.006 | PubMed

GTEx Consortium (2013) The Genotype-Tissue Expression (GTEx) project. *Nat Genet* **45**:580-585 https://doi.org/10.1038/ng.2653 | PubMed

GTEx Consortium (2017) Genetic effects on gene expression across human tissues. *Nature* **550**:204-213 https://doi.org/10.1038/nature24277 | PubMed

Gunturkun MH, Flashner E, Wang T, Mulligan MK, Williams RW, Prins P, Chen H (2022) GeneCup: mining PubMed and GWAS catalog for gene-keyword relationships. *G3* https://doi.org/10.1093/g3journal/jkac059 | PubMed

Hafemeister C, Satija R (2019) Normalization and variance stabilization of single-cell RNA-seq data using regularized negative binomial regression. *Genome Biol* **20**:296 https://doi.org/10.1186/s13059-019-1874-1 | PubMed

Hatoum AS, Colbert SMC, Johnson EC, Huggett SB, Deak JD, Pathak GA, Jennings MV, Paul SE, Karcher NR, Hansen I, *et al.* (2022a) Multivariate genome-wide association meta-analysis of over 1 million subjects identifies loci underlying multiple substance use disorders. *bioRxiv* https://doi.org/10.1101/2022.01.06.22268753

Hatoum AS, Johnson EC, Colbert SMC, Polimanti R, Zhou H, Walters RK, Gelernter J, Edenberg HJ, Bogdan R, Agrawal A (2022b) The addiction risk factor: A unitary genetic vulnerability characterizes substance use disorders and their associations with common correlates. *Neuropsychopharmacology* **47**:1739-1745 https://doi.org/10.1038/s41386-021-01209-w | PubMed

Hu C, Tao L, Cao X, Chen L (2020) The solute carrier transporters and the brain: Physiological and pharmacological implications. *Asian J Pharm Sci* **15**:131-144 https://doi.org/10.1016/j.ajps.2019.09.002 | PubMed

Hurkmans EGE, Koenderink JB, van den Heuvel JJMW, Versleijen-Jonkers YMH, Hillebrandt-Roeffen MHS, Groothuismink JM, Vos HI, van der Graaf WTA, Flucke U, Muradjan G, *et al.* (2022) SLC7A8 coding for LAT2 is associated with early disease progression in osteosarcoma and transports doxorubicin. *Front Pharmacol* **13**:1042989 https://doi.org/10.3389/fphar.2022.1042989 | PubMed

Karlsson R-M, Hefner KR, Sibley DR, Holmes A (2008) Comparison of dopamine D1 and D5 receptor knockout mice for cocaine locomotor sensitization. *Psychopharmacology* **200**:117-127 https://doi.org/10.1007/s00213-008-1165-0 | PubMed

Lin L, Yee SW, Kim RB, Giacomini KM (2015) SLC transporters as therapeutic targets: emerging opportunities. *Nat Rev Drug Discov* **14**:543-560 https://doi.org/10.1038/nrd4626 | PubMed

Liu C-J, Dib-Hajj SD, Renganathan M, Cummins TR, Waxman SG (2003) Modulation of the cardiac sodium channel Nav1.5 by fibroblast growth factor homologous factor 1B. *J Biol Chem* **278**:1029-1036 https://doi.org/10.1074/jbc.m207074200 | PubMed

Mackay TFC (2014) Epistasis and quantitative traits: using model organisms to study gene-gene interactions. *Nat Rev Genet* **15**:22-33 https://doi.org/10.1038/nrg3627 | PubMed

Mague SD, Isiegas C, Huang P, Liu-Chen L-Y, Lerman C, Blendy JA (2009) Mouse model of OPRM1 (A118G) polymorphism has sex-specific effects on drug-mediated behavior. *Proc Natl Acad Sci U S A* **106**:10847-10852 https://doi.org/10.1073/pnas.0901800106 | PubMed

McCreary JK, Keiko McCreary J, Sorina Truica L, Friesen B, Yao Y, Olson DM, Kovalchuk I, Cross AR, Metz GAS (2016) Altered brain morphology and functional connectivity reflect a vulnerable affective state after cumulative multigenerational stress in rats. *Neuroscience* https://doi.org/10.1016/j.neuroscience.2016.05.046 | PubMed

McGinnis CS, Murrow LM, Gartner ZJ (2019) DoubletFinder: Doublet Detection in Single-Cell RNA Sequencing Data Using Artificial Nearest Neighbors. *Cell Syst* **8**:329-337. https://doi.org/10.1016/j.cels.2019.03.003 | PubMed

Mohammadnejad A, Nygaard M, Li S, Zhang D, Xu C, Li W, Lund J, Christiansen L, Baumbach J, Christensen K, *et al.* (2020) Generalized correlation coefficient for genome-wide association analysis of cognitive ability in twins. *Aging* **12**:22457-22494 https://doi.org/10.18632/aging.104198 | PubMed

Mori T, Ito S, Narita M, Suzuki T, Sawaguchi T (2004) Combined effects of psychostimulants and morphine on locomotor activity in mice. *J Pharmacol Sci* **96**:450-458 https://doi.org/10.1254/jphs.fpj04039x | PubMed

Mulligan MK, Mozhui K, Prins P, Williams RW (2017) GeneNetwork: A Toolbox for Systems Genetics. In: Schughart K, Williams RW (Eds). *Systems Genetics: Methods and Protocols* New York, NY: Springer New York. pp. 75-120 https://doi.org/10.1007/978-1-4939-6427-7_4 | PubMed

Murphy NP, Lam HA, Maidment NT (2001) A comparison of morphine-induced locomotor activity and mesolimbic dopamine release in C57BL6, 129Sv and DBA2 mice. *J Neurochem* **79**:626-635 https://doi.org/10.1046/j.1471-4159.2001.00599.x | PubMed

Nelson EC, Agrawal A, Heath AC, Bogdan R, Sherva R, Zhang B, Al-Hasani R, Bruchas MR, Chou Y-L, Demers CH, *et al.* (2016) Evidence of CNIH3 involvement in opioid dependence. *Mol Psychiatry* **21**:608-614 https://doi.org/10.1038/mp.2015.102 | PubMed

O'Leary NA, Wright MW, Rodney Brister J, Ciufo S, Haddad D, McVeigh R, Rajput B, Robbertse B, Smith-White B, Ako-Adjei D, *et al.* (2016) Reference sequence (RefSeq) database at NCBI: current status, taxonomic expansion, and functional annotation. *Nucleic Acids Research* https://doi.org/10.1093/nar/gkv1189 | PubMed

Philip VM, Duvvuru S, Gomero B, Ansah TA, Blaha CD, Cook MN, Hamre KM, Lariviere WR, Matthews DB, Mittleman G, *et al.* (2010) High-throughput behavioral phenotyping in the expanded panel of BXD recombinant inbred strains. *Genes Brain Behav* **9**:129-159 https://doi.org/10.1111/j.1601-183x.2009.00540.x | PubMed

Popova D, Desai N, Blendy JA, Pang ZP (2019) Synaptic Regulation by OPRM1 Variants in Reward Neurocircuitry. *J Neurosci* **39**:5685-5696 https://doi.org/10.1523/jneurosci.2317-18.2019 | PubMed

Sanchez-Roige S, Fontanillas P, Jennings MV, Bianchi SB, Huang Y, Hatoum AS, Sealock J, Davis LK, Elson SL, Palmer AA. (2021) Genome-wide association study of problematic opioid prescription use in 132,113 23andMe research participants of European ancestry. *Mol Psychiatry* **26**:6209-6217 https://doi.org/10.1038/s41380-021-01335-3 | PubMed

Savell KE, Tuscher JJ, Zipperly ME, Duke CG, Phillips RA, Bauman AJ, Thukral S, Sultan FA, Goska NA, Ianov L, *et al.* (2020) A dopamine-induced gene expression signature regulates neuronal function and cocaine response. *Sci Adv* **6**:eaba4221 https://doi.org/10.1126/sciadv.aba4221 | PubMed

Schoorlemmer J, Goldfarb M (2001) Fibroblast growth factor homologous factors are intracellular signaling proteins. *Curr Biol* **11**:793-797 https://doi.org/10.1016/s0960-9822(01)00232-9 | PubMed

Seiffert S, Pendziwiat M, Bierhals T, Goel H, Schwarz N, van der Ven A, Boßelmann CM, Lemke J, Syrbe S, Willemsen MH, *et al.* (2022) Modulating effects of FGF12 variants on NaV1.2 and NaV1.6 being associated with developmental and epileptic encephalopathy and Autism spectrum disorder: A case series. *EBioMedicine* **83**:104234 https://doi.org/10.1016/j.ebiom.2022.104234 | PubMed

Severino AL, Mittal N, Hakimian JK, Velarde N, Minasyan A, Albert R, Torres C, Romaneschi N, Johnston C, Tiwari S, *et al.* (2020) μ-Opioid Receptors on Distinct Neuronal Populations Mediate Different Aspects of Opioid Reward-Related Behaviors. *eNeuro* **7** https://doi.org/10.1523/ENEURO.0146-20.2020 | PubMed

Singh AK, Bernabucci M, Dvorak NM, Haghighijoo Z, Di Re J, Goode NA, Kadakia FK, Maile LA, Folorunso OO, Wadsworth PA, *et al.* (2025) Sensory neuron-expressed FGF13 controls nociceptive signaling in diabetic neuropathy models. *J Clin Invest* **135** https://doi.org/10.1172/JCI183749 | PubMed

Sloan Z, Arends D, Broman K W., Centeno A, Furlotte N, Nijveen H, Yan L, Zhou X, Williams R W., Prins P (2016) GeneNetwork: framework for web-based genetics. *J Open Source Softw* **1**:25 https://doi.org/10.21105/joss.00025

Smith MA, Greene-Naples JL, Lyle MA, Iordanou JC, Felder JN (2009) The effects of repeated opioid administration on locomotor activity: I. Opposing actions of mu and kappa receptors. *J Pharmacol Exp Ther* **330**:468-475 https://doi.org/10.1124/jpet.108.150011 | PubMed

Sochacka M, Opalinski L, Szymczyk J, Zimoch MB, Czyrek A, Krowarsch D, Otlewski J, Zakrzewska M (2020) FHF1 is a bona fide fibroblast growth factor that activates cellular signaling in FGFR-dependent manner. *Cell Commun Signal* **18**:69 https://doi.org/10.1186/s12964-020-00573-2 | PubMed

Stertz L, Di Re J, Pei G, Fries GR, Mendez E, Li S, Smith-Callahan L, Raventos H, Tipo J, Cherukuru R, *et al.* (2021) Convergent genomic and pharmacological evidence of PI3K/GSK3 signaling alterations in neurons from schizophrenia patients. *Neuropsychopharmacology* **46**:673-682 https://doi.org/10.1038/s41386-020-00924-0 | PubMed

Stuart T, Butler A, Hoffman P, Hafemeister C, Papalexi E, Mauck WM, Hao Y, Stoeckius M, Smibert P, Satija R. (2019) Comprehensive Integration of Single-Cell Data. *Cell* **177**:1888-1902. https://doi.org/10.1016/j.cell.2019.05.031 | PubMed

Theriot J, Sabir S, Azadfard M. (2022) *Opioid AntagonistsStatPearls* Treasure Island (FL): StatPearls Publishing.

Torrents D, Estévez R, Pineda M, Fernández E, Lloberas J, Shi YB, Zorzano A, Palacín M (1998) Identification and characterization of a membrane protein (y+L amino acid transporter-1) that associates with 4F2hc to encode the amino acid transport activity y+L. A candidate gene for lysinuric protein intolerance. *J Biol Chem* **273**:32437-32445 https://doi.org/10.1074/jbc.273.49.32437 | PubMed

Torrents D, Mykkänen J, Pineda M, Feliubadaló L, Estévez R, de Cid R, Sanjurjo P, Zorzano A, Nunes V, Huoponen K, *et al.* (1999) Identification of SLC7A7, encoding y+LAT-1, as the lysinuric protein intolerance gene. *Nat Genet* **21**:293-296 https://doi.org/10.1038/6809 | PubMed

Uffelmann E, Huang QQ, Munung NS, de Vries J, Okada Y, Martin AR, Martin HC, Lappalainen T. (2021) Genome-wide association studies. *Nature Reviews Methods Primers* **1**:1-21 https://doi.org/10.1038/s43586-021-00056-9

Velásquez VB, Zamorano GA, Martínez-Pinto J, Bonansco C, Jara P, Torres GE, Renard GM, Sotomayor-Zárate R (2019) Programming of Dopaminergic Neurons by Early Exposure to Sex Hormones: Effects on Morphine-Induced Accumbens Dopamine Release, Reward, and Locomotor Behavior in Male and Female Rats. *Front Pharmacol* **10**:295 https://doi.org/10.3389/fphar.2019.00295 | PubMed

Wang YP, Wei SG, Zhu YS, Zhao B, Xun X, Lai JH (2015) Dopamine receptor D1 but not D3 essential for morphine-induced conditioned responses. *Genet Mol Res* **14**:180-189 https://doi.org/10.4238/2015.january.16.1 | PubMed

Watson PM, Ashbrook DG (2020) GeneNetwork: a continuously updated tool for systems genetics analyses. *bioRxiv* https://doi.org/10.1101/2020.12.23.424047

Wei W-H, Hemani G, Haley CS (2014) Detecting epistasis in human complex traits. *Nat Rev Genet* **15**:722-733 https://doi.org/10.1038/nrg3747 | PubMed

Wildburger NC, Ali SR, Hsu W-CJ, Shavkunov AS, Nenov MN, Lichti CF, LeDuc RD, Mostovenko E, Panova-Elektronova NI, Emmett MR, *et al.* (2015) Quantitative proteomics reveals protein-protein interactions with fibroblast growth factor 12 as a component of the voltage-gated sodium channel 1.2 (nav1.2) macromolecular complex in Mammalian brain. *Mol Cell Proteomics* **14**:1288-1300 https://doi.org/10.1074/mcp.m114.040055 | PubMed

Williams RW, Gu J, Qi S, Lu L (2001) The genetic structure of recombinant inbred mice: high-resolution consensus maps for complex trait analysis. *Genome Biol* **2**:RESEARCH0046 https://doi.org/10.1186/gb-2001-2-11-research0046 | PubMed

Xu M, Hu XT, Cooper DC, Moratalla R, Graybiel AM, White FJ, Tonegawa S (1994) Elimination of cocaine-induced hyperactivity and dopamine-mediated neurophysiological effects in dopamine D1 receptor mutant mice. *Cell* **79**:945-955 https://doi.org/10.1016/0092-8674(94)90026-4 | PubMed

Yam MF, Loh YC, Tan CS, Khadijah Adam S, Abdul Manan N, Basir R (2018) General Pathways of Pain Sensation and the Major Neurotransmitters Involved in Pain Regulation. *Int J Mol Sci* **19** https://doi.org/10.3390/ijms19082164 | PubMed

Zhang B, Kirov S, Snoddy J (2005) WebGestalt: an integrated system for exploring gene sets in various biological contexts. *Nucleic Acids Res* **33**:W741-8 https://doi.org/10.1093/nar/gki475 | PubMed

Zhang L, Zhang J-T, Hang L, Liu T (2020) Mu Opioid Receptor Heterodimers Emerge as Novel Therapeutic Targets: Recent Progress and Future Perspective. *Front Pharmacol* **11**:1078 https://doi.org/10.3389/fphar.2020.01078 | PubMed

Zhou H, Rentsch CT, Cheng Z, Kember RL, Nunez YZ, Sherva RM, Tate JP, Dao C, Xu K, Polimanti R, *et al.* (2020) Association of OPRM1 Functional Coding Variant With Opioid Use Disorder: A Genome-Wide Association Study. *JAMA Psychiatry* **77**:1072-1080 https://doi.org/10.1001/jamapsychiatry.2020.1206 | PubMed

Zhou X, Stephens M (2012) Genome-wide efficient mixed-model analysis for association studies. *Nat Genet* **44**:821-824 https://doi.org/10.1038/ng.2310 | PubMed

Ziebarth JD, Cui Y (2017) Precise Network Modeling of Systems Genetics Data Using the Bayesian Network Webserver. *Methods Mol Biol* **1488**:319-335 https://doi.org/10.1007/978-1-4939-6427-7_15 | PubMed

Zuo Y, Telese F, Chen H (2023) Opiate responses are controlled by interactions of Oprm1 and Fgf12 loci in the murine BXD family: Correspondence to human GWAS findings. NCBI Gene Expression Omnibus. ID GSE214388 https://www.ncbi.nlm.nih.gov/geo/query/acc.cgi?acc=GSE214388

Philip VM, Duvvuru S, et al (2010) Central nervous system, pharmacology, behavior: Morphine response (50 mg/kg ip) and naloxone response (30 mg/kg ip),. genenetwork. ID www.genenetwork.org www.genenetwork.org

Peer reviews

Reviewer #1 (Public review):

[Editors' note: this version has been assessed by the Reviewing Editor without further input from the original reviewers. The authors have appropriately addressed the comments raised in the previous round of review.]

Summary:

The study by Lemen et al. represents a comprehensive and unique analysis of gene networks in rat models of opioid use disorder, using multiple strains and both sexes. It provides a time-series analysis of Quantitative Trait Loci (QTLs) in response to morphine exposure.

Strengths:

A key finding is the identification of a previously unknown morphine-sensitive pathway involving Oprm1 and Fgf12, which activates a cascade through MAPK kinases in D1 medium spiny neurons (MSNs). Strengths include the large-scale, multi-strain, sex-inclusive design, the time-series QTL mapping provides dynamic insights, and the discovery of an Oprm1-Fgf12-MAPK signaling pathway in D1 MSNs, which is novel and relevant.

https://doi.org/10.7554/eLife.108845.2.sa3

Reviewer #2 (Public review):

Summary:

This highly novel and significant manuscript re-analyzes behavioral QTL data derived from morphine locomotor activity in the BXD recombinant inbred panel. The combination of interacting behavioral-pharmacology (morphine and naltrexone) time course data, high-resolution mouse genetic analyses, genetic analysis of gene expression (eQTLs), cross-species analysis with human gene expression and genetic data, and molecular modeling approaches with Bayesian network analysis produces new information on loci modulating morphine locomotor activity.

Furthermore, the identification of time-wise epistatic interactions between the Oprm1 and Fgf12 loci is highly novel and points to methodological approaches for identifying other epistatic interactions using animal model genetic studies.

Strengths:

(1) Use of state-of-the art genetic tools for mapping behavioral phenotypes in mouse models.

(2) Adequately powered analysis incorporating both sexes and time course analyses.

(3) Detection of time and sex-dependent interactions of two QTL loci modulating morphine locomotor activity.

(4) Identification of putative candidate genes by combined expression and behavioral genetic analyses.

(5) Use of Bayesian analysis to model causal interactions between multiple genes and behavioral time points.

Appraisal:

The authors largely succeeded in reaching goals with novel findings and methodology.

Significance of Findings:

This study will likely spur future direct experimental studies to test hypotheses generated by this complex analysis. Additionally, the broad methodological approach incorporating time course genetic analyses may encourage other studies to identify epistatic interactions in mouse genetic studies.

https://doi.org/10.7554/eLife.108845.2.sa2

Reviewer #3 (Public review):

Summary:

This is a clearly written paper that describes the reanalysis of data from a BXD study of the locomotor response to morphine and naloxone. The authors detect significant loci and an epistatic interaction between two of those loci. Single-cell data from outbred rats is used to investigate the interaction. The authors also use network methods and incorporate human data into their analysis.

Strengths:

One major strength of this work is the use of granular time-series data, enabling the identification of time-point-specific QTL. This allowed for the identification of an additional, distinct QTL (the Fgf12 locus) in this work compared to previously published analysis of these data, as well as the identification of an epistatic effect between Oprm1 (driving early stages of locomotor activation) and Fgf12 (driving later stages).

https://doi.org/10.7554/eLife.108845.2.sa1

Author response:

The following is the authors' response to the original reviews.

> ***Public Reviews:***
>
> ***Reviewer #1 (Public review):***
>
> *Summary:*
>
> *The study by Lemen et al. represents a comprehensive and unique analysis of gene networks in rat models of opioid use disorder, using multiple strains and both sexes. It provides a time-series analysis of Quantitative Trait Loci (QTLs) in response to morphine exposure.*
>
> *Strengths:*
>
> *A key finding is the identification of a previously unknown morphine-sensitive pathway involving Oprm1 and Fgf12, which activates a cascade through MAPK kinases in D1 medium spiny neurons (MSNs). Strengths include the large-scale, multi-strain, sex-inclusive design, the time-series QTL mapping provides dynamic insights, and the discovery of an Oprm1-Fgf12-MAPK signaling pathway in D1 MSNs, which is novel and relevant.*
>
> *Weaknesses:*

> *(1) The proposed involvement of Nav1.2 (SCN2A) as a downstream target of the Oprm1-Fgf12 pathway requires further analysis/evidence. Is Nav1.2 (SCN2A) expressed in D1 neurons?*
>
> *The authors mentioned that SCN8A (Nav1.6) was tested as a candidate mediator of Oprm1-Fgf12 loci and variation in locomotor activity. However, the proposed model supports SCN2A as a target rather than SCN8A. This is somewhat unexpected since SCN8A is highly abundant in MSN.*
>
> *Can the authors provide expression data for SCN2A, Oprm1, and Fgf12 in D1 vs. D2 MSNs?*

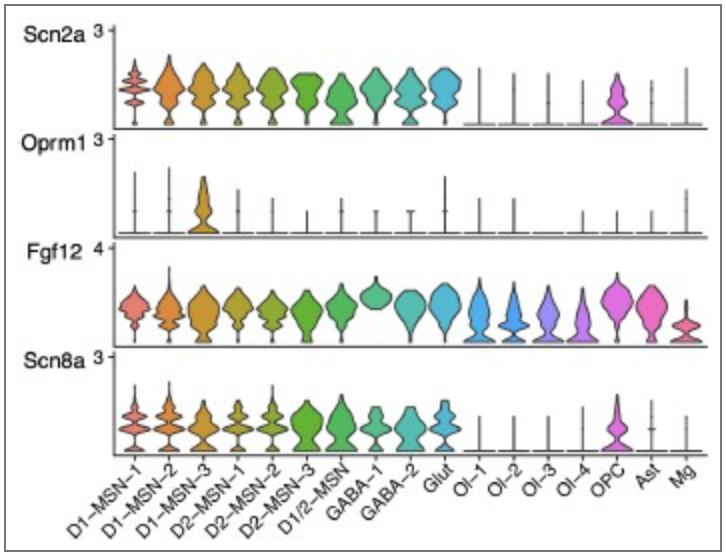

Author response image 1.

We generated Author response image 1 to show both Scn2a and Scn8a are ubiquitously expressed in MSN and GABAergic neurons.

> *(2) The authors should consider adding a reference to FGF12 in Schizophrenia (PMC8027596) in the Introduction.*

This is a relevant reference. We have cited it in the discussion section instead of introduction because we felt that is more relevant.

> *(3) There is recent evidence supporting the druggability of other intracellular FGFs, such as FGF14 (PMC11696184) and FGF13 (PMC12259270), through their interactions with Nav channels. What are the implications of these findings for drug discovery in the context of the present study? Could FGF12 be considered a potential druggable therapeutic target for opioid use disorder (OUD)?*

The recent success in targeting FGF14 and FGF13 protein-protein interactions with sodium channels suggests that FGF12 could indeed be a druggable target for OUD. We have added a section to the Discussion exploring the potential for developing small-molecule modulators of the FGF12-Nav interface as a novel therapeutic strategy.

> ***Reviewer #2 (Public review):***
>
> *Summary:*

> *This highly novel and significant manuscript re-analyzes behavioral QTL data derived from morphine locomotor activity in the BXD recombinant inbred panel. The combination of interacting behavioral-pharmacology (morphine and naltrexone) time course data, high-resolution mouse genetic analyses, genetic analysis of gene expression (eQTLs), cross-species analysis with human gene expression and genetic data, and molecular modeling approaches with Bayesian network analysis produces new information on loci modulating morphine locomotor activity.*
>
> *Furthermore, the identification of time-wise epistatic interactions between the Oprm1 and Fgf12 loci is highly novel and points to methodological approaches for identifying other epistatic interactions using animal model genetic studies.*
>
> *Strengths:*
>
> *(1) Use of state-of-the art genetic tools for mapping behavioral phenotypes in mouse models.*
>
> *(2) Adequately powered analysis incorporating both sexes and time course analyses.*
>
> *(3) Detection of time and sex-dependent interactions of two QTL loci modulating morphine locomotor activity.*
>
> *(4) Identification of putative candidate genes by combined expression and behavioral genetic analyses.*
>
> *(5) Use of Bayesian analysis to model causal interactions between multiple genes and behavioral time points.*
>
> *Weaknesses:*
>
> *(1) There is a need for careful editing of the text and figures to eliminate multiple typographical and other compositional errors.*

We have performed a thorough review of the manuscript and corrected typographical errors, including "ddactivates" and other compositional issues.

> *(2) There are multiple examples of overstating the possible significance of results that should be corrected or at least directly pointed out as weaknesses in the Discussion. These include:*
>
> *(a) Assumption that the Oprm1 gene is the causal candidate gene for the major morphine locomotor Chr10 QTL at the early time epochs. Oprm1 is 400,000 bp away from the support interval of the Mor10a QTL locus, and there is no mention as to whether the Oprm1 mRNA eQTL overlaps with Mor10a.*

We have clarified this in the text. While *Oprm1* is located proximal to the peak, its massive size and the presence of a strong mRNA cis-eQTL in the NAc and hippocampus that precisely overlaps with the *Mor10a* QTL support interval provide robust evidence for its candidacy. We have added this detail to the Results section.

> *(b) Although the Bayesian analysis of possible complex interactions between Oprm1, Fgf12, other interacting genes, and behaviors is very innovative and produces testable hypotheses, a more straightforward mediation analysis of causal relationships between genotype, gene expression, and phenotype would have added strength to the arguments for the causal role of these individual genes.*

We agree that mediation analysis would be a valuable addition. We revised the Results section to acknowledge that while the Bayesian network provides a comprehensive causal

hypothesis, future studies employing formal mediation analysis could further strengthen these individual gene-to-behavior links.

> *(c) The GWAS data analysis for Oprm1 and Fgf12 is incomplete in not mentioning actual significance levels for Oprm1 and perhaps overstating the nominal significance findings for Fgf12.*

We have updated the manuscript to include the specific significance levels for the human GWAS findings related to *Oprm1* and *Fgf12*. We have clarified that the *OPRM1* variant rs1799971 reached genome-wide significance (OR = 1.046, $p = 4.92 \times 10^{-9}$). Furthermore, we have ensured that the findings for *FGF12* are described as nominally significant to avoid any overstatement of the results. For example, we now specify that the top *FGF12* SNP rs1553460 achieved nominal significance (OR = 1.015, $p = 0.021$). The Results and Discussion sections have been revised to reflect these precise statistical values.

> *Appraisal:*
>
> *The authors largely succeeded in reaching goals with novel findings and methodology.*
>
> *Significance of Findings:*
>
> *This study will likely spur future direct experimental studies to test hypotheses generated by this complex analysis. Additionally, the broad methodological approach incorporating time course genetic analyses may encourage other studies to identify epistatic interactions in mouse genetic studies.*
>
> ***Reviewer #3 (Public review):***
>
> *Summary:*
>
> *This is a clearly written paper that describes the reanalysis of data from a BXD study of the locomotor response to morphine and naloxone. The authors detect significant loci and an epistatic interaction between two of those loci. Single-cell data from outbred rats is used to investigate the interaction. The authors also use network methods and incorporate human data into their analysis.*
>
> *Strengths:*
>
> *One major strength of this work is the use of granular time-series data, enabling the identification of time-point-specific QTL. This allowed for the identification of an additional, distinct QTL (the Fgf12 locus) in this work compared to previously published analysis of these data, as well as the identification of an epistatic effect between Oprm1 (driving early stages of locomotor activation) and Fgf12 (driving later stages).*
>
> *Weaknesses:*
>
> *(1) What criteria were used to determine whether the epistatic interaction was significant? How many possible interactions were explored?*

By design we only tested for epistasis between the Oprm1 and the Fgf12 loci—a single test of a non-linear interaction. As such there is no correction for multiple tests and no need for permutation. In other words the "nominal" P value in this case is the only relevant P value. We have added this clarification in the Results and Methods.

> *(2) Results are presented for males and females separately, but the decision to examine the two sexes separately was never explained or justified. Since it is not standard to perform GWAS broken down by sex, some initial explanation of this decision is needed. Perhaps the discussion could also discuss what (if anything) was learned as a result of the sex-specific analysis. In the end, was it useful?*

We chose to analyze sexes separately AND jointly due to significant sex differences and sex by strain interactions in locomotion data. This rationale has been added to the results section. We also discussed sex-specific results in the revision.

> *(3) The confidence intervals for the results were not well described, although I do see them in one of the tables. The authors used a 1.5 support interval, but didn't offer any justification for this decision. Is that a 95% confidence interval? If not, should more consideration have been given to genes outside that interval? For some of the QTLs that are not the focus of this paper, the confidence intervals were very large (>10 Mb). Is that typical for BXDs?*

The 1.5 LOD support interval is a standard metric for most QTL mapping studies, and does correspond approximately to a 95% confidence or support interval. Large intervals are common in BXD studies when effect sizes are moderate or recombination density is lower in specific regions. We have clarified the use of the 1.5 LOD interval in the Results section.

> ***Recommendations for the authors:***
>
> ***Reviewer #1 (Recommendations for the authors):***
>
> *In the vast majority of the figures, the text is too small to read.*

We have adjusted the font size in most of the figures.

> ***Reviewer #2 (Recommendations for the authors):***
>
> *(1) There is a need for careful editing of the text and figures to eliminate multiple typographical and other compositional errors. Examples of these include:*
>
> *(a) Figure 2E&F lacks identification of Oprm1 as the gene for cis-eQTL studies.*
>
> *(b) Figure 2H is fairly uninterpretable given the small font sizes. It should be excluded, put as a supplemental figure, or reconfigured to highlight the most important findings in a more legible manner.*
>
> *(c) Figure 4b: columns in the table need to be identified by a header row.*

We thank the reviewer for these comments and have addressed them in the revised version.

Oprm1 is now labeled in Figure 2E and 2F, Figure 2G and 2H is now moved to the Supplementary material. And a header row is added to the table in Figure 4b.

> ***Reviewer #3 (Recommendations for the authors):***
>
> *Abstract*
>
> *(1) For the abstract, it might be simpler to name the alleles as "the C57BL/6J allele", etc., since B allele will confuse people unfamiliar with mouse nomenclature.*

It is critical to not confound the organism known as C57BL/6J with the genotype, allele, or haplotype that a mouse happens to inherit. Diverse types of mice inherit reference alleles but they may be only very distantly related the C57BL/6J strain. And even the C57BL/6J strain is a moving target that accumulates mutations that are not even consider reference. For example

the mutation in Gabra2 of C57BL/6J is a de novo mutation that is not carried by many of the BXD strains since this mutation happened in JAX foundation stock after the BXDs were first established by Dr. Ben Taylor in the 1970s.

The convention is to refer to mouse strains by one string and RRID, the abbreviation of that strain by a common code (often B6), and the abbreviation of the allele, genotype, or haplotype by the italic letter *B*. This has been the recommendation of the Mouse Nomenclature Committee (on which one of the authors has been a member) for well over 50 years.

> *(2) I wondered if "also associated with a high B allele" could be reworded somehow; I had to re-read that sentence several times.*

This sentence has been reworded for clarity.

> *(3) Parts of the abstract are written in the present tense, but then it switches to past ("we generated" but then "a Bayesian network analysis supports...").*

We have thoroughly revised the abstract. Following standard scientific writing conventions, we now utilize the past tense to describe the specific experimental actions and results of this study. We have maintained the present tense for established biological facts and the broader significance of the findings.

> *(4) While the -log(p) values are all impressive, the abstract should indicate what threshold is used for genome-wide significance and how that threshold was obtained.*

We have added the significance threshold to the Abstract.

> *(5) Do the details of the MAP kinase cascade need to be explained in the abstract? It feels like a lot of detail for an abstract and represents one of the most speculative aspects of the paper. Maybe just say you identified a possible network, but save the details for the main paper.*

This is a valid suggestion. We removed the specific MAP kinase from the abstract.

> *Introduction*
>
> *(1) You could add a sentence explaining why using an LMM (GEMMA) was an improvement over the prior analysis.*

We have added a sentence explaining that GEMMA improves mapping power and better controls for population structure compared to previous methods.

> *(2) When mentioning Philips 2010, you could indicate that it identified Oprm1. This might be easier than "In addition to Oprm1" which confused me at first because it had not been mentioned before, so 'in addition' was jarring.*

We have revised the text to state that Philip et al. (2010) originally identified the *Oprm1* locus.

> *Results*
>
> *(1) There are additional instances of the tense switching between past and present in the results section.*

We have standardized the tenses in the Results section.

> *(2) "Ostn, Uts2d, Ccdc50, Gm10823, Fgf12, and Mb21d2" - before giving arguments for fgf12, can you clarify if there are coding variants or eQTLs for any of these genes?*

We have added a statement clarifying the coding variants for other genes in this interval and highlighting their eQTL status.

> *(3) "a total number of 4,495 high-quality nuclei transcriptomes". Consider removing the word "number".*

Removed.

> *(4) "approximately 6 males and 6 females" - could you point the reader to a supplementary table that has the exact number of individuals at the end of this sentence?*

The exact number of mice used in each of the BXD strains is not recorded in the original publication by Philip et al., with only mean and max was given. We have clarified that 6 is the average.

> *(5) "computed using a subset" - please explain how you selected this subset (I assumed LD pruning, but why not be explicit. How many SNPs/markers were there originally, and how many are retained?*

We have specified that the subset of markers was selected via LD pruning to represent the genetic diversity of the BXDs.

> *(6) A few words about how the significant threshold was obtained (permutation?) are needed.*

We have clarified that the significance threshold was obtained through 1,000 permutations.

> *(7) Some of the GWAS results are presented for males and females separately (as well as combined). This is not typical, and so maybe a sentence explaining why the authors thought there might be sex specific GWAS results would be warranted.*

The rationale for sex-specific analysis is provided in the results section (significant sex difference and sex by strain interaction)

> *(8) The correlation between the sexes of 0.68 could be evidence that there are sex-specific genetic effects, but could it also just be due to increased noise as you reduce sample size? What is the confidence interval for that number? Does it include 1? Or 0? If you randomly split the dataset, rather than splitting on the basis of sex, would you obtain higher correlations? The idea of sex differences is interesting, but a bit more work is needed to clarify these concerns.*

The correlation of 0.68 (95% CI: 0.52–0.79) significantly excludes both 0 and 1. The drop from r = ~0.86 at earlier intervals suggests a biological shift rather than noise due to sample size, as n remains constant (n = ~ 6 /sex/strain) across all time points. This divergence is driven by sex-specific genetic modifiers, such as the *Fgf12* locus, which is more than twice as strong in females (LOD 10.6) as in males (LOD 4.3). We have addressed this in the revision.

> *(9) Maybe I missed it, but how did you determine the threshold for significance for the epistatic interaction? Could you also clearly indicate how many possible cases of epistasis were examined/considered, since that dictates the correction for multiple testing.*

We only tested the interaction between the *Fgf12* and the *Oprm* loci.

> *(10) "To further examine whether Oprm1 and Fgf12 were co-expressed in the same cells of the NAc," can you first give an indication as to why you looked in NAc versus other brain areas you might have considered?*

We have added a sentence explaining that the NAc was chosen due to its central role in opioid reward and the observed strain differences in dopamine release in this region.

> *(11) "...from every cell type conveyed a weak but significant positive correlation (r = 0.08, p = 1.8e-8) between the expression of Oprm1 and Fgf12 (Figure 7e). When we performed Pearson's correlation analysis within each individual cell cluster, only D1-MSN-3 had a significant positive correlation (r = 0.35, p = 6.1e-8, Figure 7f). In contrast, D1-MSN-2 had a significantly weak negative correlation (r = -0.12, p = 0.02, Figure 7g)." Can you explain why these correlations are relevant? What hypothesis are you testing?*

We have clarified that these correlations were used to test the hypothesis that *Oprm1* and *Fgf12* are co-expressed and potentially co-regulated within the same neuronal subtype to support their epistatic interaction.

> *(12) "After the morphine locomotion tests were complete," can you give a specific timepoint? Like, was it exactly 180 minutes after the morphine injection?*

We have specified that naloxone was injected exactly 180 minutes after the morphine injection.

> *(13) I appreciate the desire to relate the results of this paper to human GWAS results; however, I don't feel there is much worth discussing beyond the Oprm1 finding. Therefore, I would suggest removing this from the results section and instead just making it a discussion topic. The results presented are clearly the weakest part of this paper, and I personally think it is a shame to end the results section with something that is not very informative. But I suspect the authors may wish to retain this section, and I leave that decision to them and the editor.*

We have retained this section but moved some of the more speculative human data discussion to the Discussion section as suggested.

> *Discussion*
>
> *(1) Typo "deactivates".*

Corrected to "activates".

> *(2) The last sentence in the first paragraph again discusses the comparison to humans; I would remove this.*

That sentence is condensed.

> *(3) "These data indicate that Oprm1 is a strong candidate gene for the Chr 10 locus associated with morphine-induced locomotion response." I would remind them of the eQTL for Oprm1 since this is a key piece of evidence supporting this gene as a candidate.*

We have added a reminder of the overlapping mRNA cis-eQTL for Oprm1.

> *(4) "It is likely that differences in morphine-induced dopamine release are involved in the highly variable locomotor responses to morphine across the BXD family." I agree this might be true, but since you have no evidence to support this claim, is it worth mentioning at all?*

We have rephrased this as a hypothesis or cited relevant literature supporting this link in parental strains.

> *(5) Could you include a sentence or two about why Philip 2010 didn't find Fgf12? Lack of markers? The difference between an LM and an LMM?*

We have added an explanation that the use of a high-density WGS-based marker set and the LMM (GEMMA) allowed for the detection of this novel locus that was previously missed.

> *(6) Section titled "Cell-type specific gene expression in NAc". While this is interesting, you might also want to remind the reader that epistatic interactions do not necessarily require the genes to be expressed in the same cell or for their gene products to physically interact.*

We have added this caveat to the Discussion.

> *(7) I think the Bayesian network section is not very strong. For example, they did not compare the results for their two chosen genes to the results they might have obtained if they had chosen other genes from their QTL intervals. My guess is that those other genes might have also produced results that were equally convincing. I'm not asking them to do that, but it reflects the risk of false positive results when taking an approach like this. Nevertheless, I am guessing the authors would prefer to include this section.*

We appreciate the reviewer pointing out this possibility and agree with this concern. We have added a statement acknowledging the risk of false positives in Bayesian modeling in this context and noting that these findings are intended as testable hypotheses

> *Methods*
>
> *(1) How were the 2 HS rats selected? I had the impression that Dr. Telese's lab had access to snRNA-seq data from more than 2 HS rats.*

We have clarified that these rats were selected based on their addiction-like behavior phenotypes from a larger cohort.

> *(2) I didn't look back, but did the main paper point out that the rats are treated with oxycodone rather than morphine?*

We have clarified this distinction in the Methods section.

https://doi.org/10.7554/eLife.108845.2.sa0